Inorganic Chemistry

Article

pubs.acs.org/IC

Oxidatively Induced P−O Bond Formation through Reductive Coupling between Phosphido and Acetylacetonate, 8-Hydroxyquinolinate, and Picolinate Groups†

Andersson Arias, Juan Forniés, Consuelo Fortuño,* and Antonio Martín

Departamento de Química Inorgánica, Instituto de Síntesis Química y Catálisis Homogénea, Universidad de Zaragoza-C.S.I.C., E-50009 Zaragoza, Spain

Piero Mastrorilli,* Stefano Todisco, Mario Latronico, and Vito Gallo

Dipartimento DICATECh del Politecnico di Bari and Istituto CNR-ICCOM, Via Orabona 4, I-70125 Bari, Italy

Supporting Information

ABSTRACT: The dinuclear anionic complexes $[NBu_4][(R_F)_2M^{II}(\mu\text{-}PPh_2)_2M'^{II}(N\hat{}O)]$ ($R_F = C_6F_5$. N^O = 8-hydroxyquinolinate, hq; M = M′ = Pt **1**; Pd **2**; M = Pt, M′ = Pd, **3**. N^O = *o*-picolinate, pic; M = Pt, M′ = Pt, **4**; Pd, **5**) are synthesized from the tetranuclear $[NBu_4]_2[\{(R_F)_2Pt(\mu\text{-}PPh_2)_2M(\mu\text{-}Cl)\}_2]$ by the elimination of the bridging Cl as AgCl in acetone, and coordination of the corresponding *N*,*O*-donor ligand (**1**, **4**, and **5**) or connecting the fragments "*cis*-$[(R_F)_2M(\mu\text{-}PPh_2)_2]^{2-}$" and "M′(N^O)" (**2** and **3**). The electrochemical oxidation of the anionic complexes **1**−**5** occurring under HRMS(+) conditions gave the cations $[(R_F)_2M(\mu\text{-}PPh_2)_2M'(N\hat{}O)]^+$, presumably endowed with a M(III),M′(III) core. The oxidative addition of I_2 to the 8-hydroxyquinolinate complexes **1**−**3** triggers a reductive coupling between a PPh_2 bridging ligand and the *N*,*O*-donor chelate ligand with formation of a P−O bond and ends up in complexes of platinum(II) or palladium(II) of formula $[(R_F)_2M^{II}(\mu\text{-}I)(\mu\text{-}PPh_2)M'^{II}(P,N\text{-}PPh_2hq)]$, M = M′ = Pt **7**, Pd **8**; M = Pt, M′ = Pd, **9**. Complexes **7**−**9** show a new $Ph_2P\text{-}OC_9H_6N$ (Ph_2P-hq) ligand bonded to the metal center in a *P*,*N*-chelate mode. Analogously, the addition of I_2 to solutions of the *o*-picolinate complexes **4** and **5** causes the reductive coupling between a PPh_2 bridging ligand and the starting *N*,*O*-donor chelate ligand with formation of a P−O bond, forming $Ph_2P\text{-}OC_6H_4NO$ (Ph_2P-pic). In these cases, the isolated derivatives $[NBu_4][(Ph_2P\text{-pic})(R_F)Pt^{II}(\mu\text{-}I)(\mu\text{-}PPh_2)M^{II}(R_F)I]$ (M = Pt **10**, Pd **11**) are anionic, as a consequence of the coordination of the resulting new phosphane ligand (Ph_2P-pic) as monodentate *P*-donor, and a terminal iodo group to the M atom. The oxidative addition of I_2 to $[NBu_4][(R_F)_2Pt^{II}(\mu\text{-}PPh_2)_2Pt^{II}(acac)]$ (**6**) (acac = acetylacetonate) also results in a reductive coupling between the diphenylphosphanido and the acetylacetonate ligand with formation of a P−O bond and synthesis of the complex $[NBu_4][(R_F)_2Pt^{II}(\mu\text{-}I)(\mu\text{-}PPh_2)Pt^{II}(Ph_2P\text{-acac})I]$ (**12**). The transformations of the starting complexes into the products containing the P−O ligands passes through mixed valence M(II),M′(IV) intermediates which were detected, for M = M′ = Pt, by spectroscopic and spectrometric measurements.

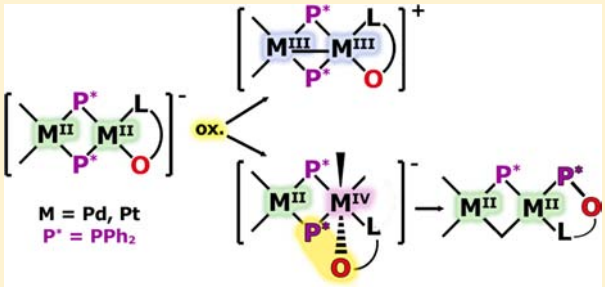

INTRODUCTION

Although the chemistry of platinum and palladium is usually studied in tandem and complexes in high oxidation states (III and IV) have been well recognized for platinum, the chemistry of palladium in oxidation states higher than (II) has been investigated in detail in the last 10 years.[2−10] These oxidized species easily undergo reductive elimination and play a key role as intermediates in some synthetic design.[11−18] The M(II)/M(IV) cycles can achieve transformations that are hardly accessible otherwise. The usual access to the M(IV) complexes is the oxidation of M(II) derivatives, and it is well established that the oxidation of dinuclear derivatives can afford M(III),M(III) or M(II),M(IV) complexes.[19−32]

In our current research on phosphanido derivatives, we have reported three types of palladium or platinum(II) dinuclear complexes $[(R_F)_2M(\mu\text{-}PPh_2)_2M'L_2]^{n-}$ ($R_F = C_6F_5$, M, M′ = Pt, Pd; L = R_F, *n* = 2, **A**; 2L = benzoquinolinate (C^N), *n* = 1, **B**; L = $NCCH_3$, *n* = 0, **C**). The two R_F groups bonded to a metal center in these complexes can act as terminal blocking ligands as well as provide adittional structural information (^{19}F NMR). The oxidation of these types of compounds with I_2 (Chart 1) has been reported.[33−35] In all cases, the oxidized intermediate

†Polynuclear Homo- or Heterometallic Palladium(II)−Platinum(II) Pentafluorophenyl Complexes Containing Bridging Diphenylphosphido Ligands. 31. For part 30, see ref 1.

Received: February 18, 2013
Published: April 18, 2013

Chart 1

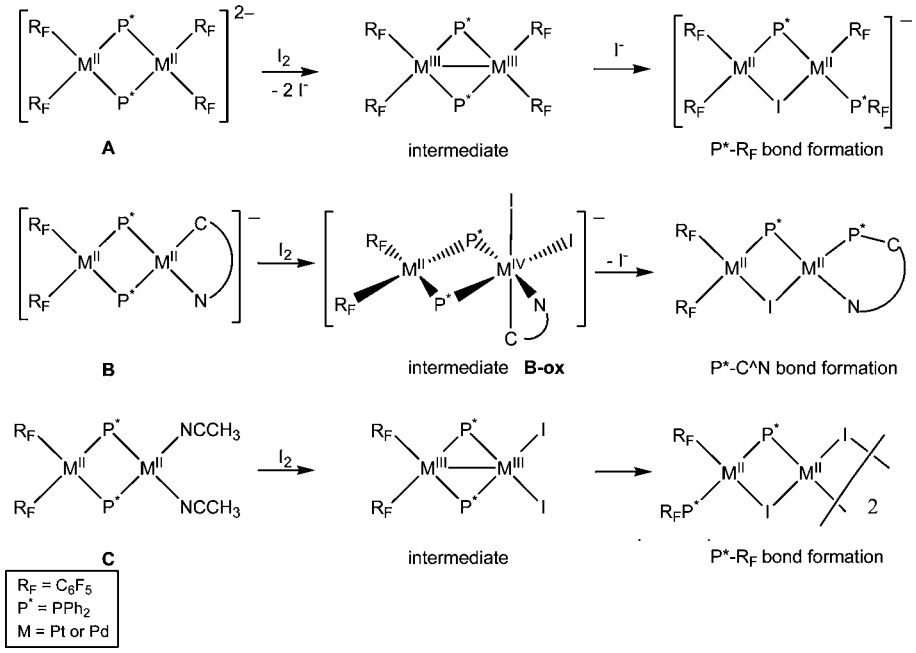

Chart 2

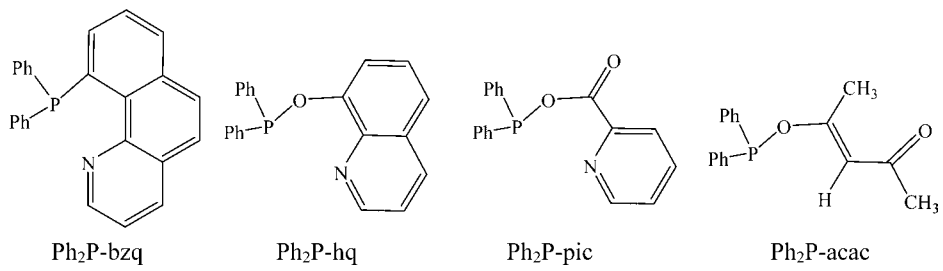

Scheme 1

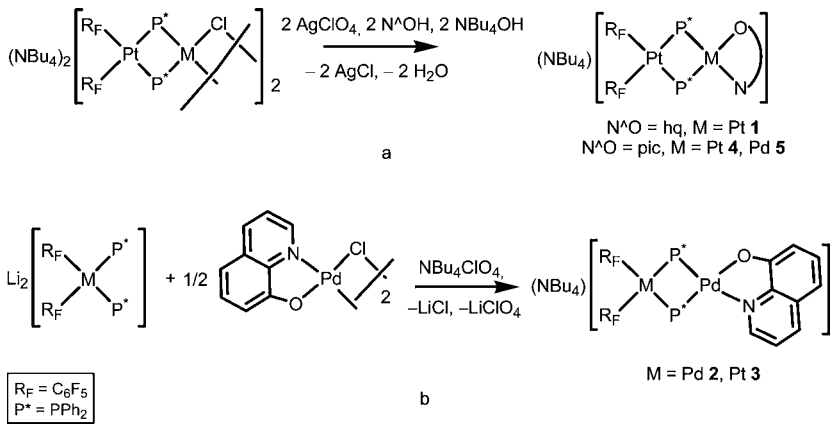

complexes evolve through a reductive coupling with formation of a P–C bond and new palladium(II) and platinum(II) derivatives. For complexes of type **A** (Chart 1), the reductive coupling between PPh_2 and C_6F_5 groups and formation of complexes containing the $PPh_2C_6F_5$ ligand was observed.[33] Only the platinum intermediate M(III),M(III) derivative, $[(R_F)_2Pt^{III}(\mu\text{-}PPh_2)_2Pt^{III}(R_F)_2]$(Pt–Pt), was stable enough, isolated and characterized.[33,36] For complexes of type **B**, the oxidation in the case of the Pt(II),Pt(II) derivative results in the formation of the diplatinum Pt(II),Pt(IV) $[NBu_4][(R_F)_2Pt^{II}(\mu\text{-}PPh_2)_2Pt^{IV}(C\text{^}N)I_2]$[34] (**B-ox**) complex which was stable enough and could be isolated and fully characterized. However, for the Pd(II),Pd(II) or the mixed Pt(II),Pd(II) complexes, the intermediates M(II),M(IV) could neither be isolated nor observed in solution, and the M(II),M(II) complexes containing the aminophosphane Ph_2P-bzq (P–C coupling, see Chart 2) were obtained. Finally, the formation of $Ph_2PC_6F_5$ was observed for the neutral complexes type **C** through the isolated and characterized intermediates of palladium or platinum(III) $[(R_F)_2Pt^{III}(\mu\text{-}PPh_2)_2M^{III}I_2]$(Pt-M) (M = Pt,

Table 1. ^{31}P and ^{195}Pt NMR Data of 1−5 and 7−12 in Deuteroacetone at 298 K[a]

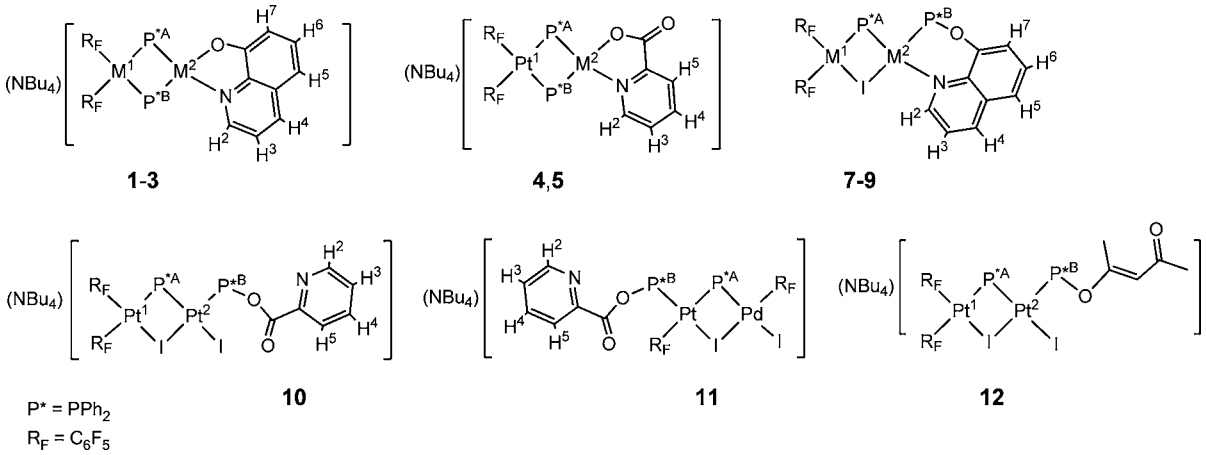

complex	δP^A	δP^B	$^2J_{P^A,P^B}$	$^1J_{P^A,Pt^1}$	$^1J_{P^A,Pt^2}$	$^1J_{P^B,Pt^1}$	$^1J_{P^B,Pt^2}$	δPt^1	δPt^2
1[b]	−137.2	−140.4	157	1892	2436	1876	2441	−3903	−3450
2	−100.4	−106.0	263						
3	−119.0	−124.5	216	1739		1719		−3901	
4[c]	−139.1	−141.6	160	1900	2420	1903	2532	−3911	−3542
5	−121.2	−125.6	220	1766		1737		−3905	
7[d]	−19.9	86.0		1903	2373	49	5025	−4250	−4420
8	55.4	122.9	32						
9	50.1	119.3	37	1928		119		−4317	
10[e]	−71.3	80.6		2005	2215		5179	−4045	−3572
10-hydr	−76.4	67.2	13	2042	2320		5019	−4050	−3520
11	−45.8	84.6	8	1654			5088	−4436	
12[f]	−88.5	81.6	21	2030	2291	29	5216	−4020	−3500

[a] δ in ppm, J in Hz. [b] $^2J_{Pt1,Pt2}$ = 289 Hz. [c] $^2J_{Pt1,Pt2}$ = 284 Hz. [d] $^2J_{Pt1,Pt2}$ = 1220 Hz. [e] $^2J_{Pt1,Pt2}$ = 1280 Hz. [f] $^2J_{Pt1,Pt2}$ = 1283 Hz.

Pd).[35] The analysis of the results indicated that (i) the reductive coupling is usually preferred on a palladium rather than on a platinum center; (ii) the coupling between PPh_2 and benzoquinolinate groups are preferred to the coupling between PPh_2 and C_6F_5 groups; (iii) in the iodo derivatives, the coupling between PPh_2 and I to form iodophosphane has not yet been observed.

In this paper we report on the synthesis of new dinuclear anionic phosphanido derivatives of platinum and palladium(II) containing 8-hydroxyquinolinate or *o*-picolinate as ligands, and the reaction of the complexes $[NBu_4][(R_F)_2Pt(\mu\text{-}PPh_2)_2M^{II}(L\text{-}L')]$ [M = Pt, Pd; L-L′ = 8-hydroxyquinolinate (hq), *o*-picolinate (pic) or acetylacetonate (acac)] with I_2.

■ RESULTS AND DISCUSSION

Synthesis of $[NBu_4][(R_F)_2M(\mu\text{-}PPh_2)_2M'(N^\wedge O)]$ (R_F = C_6F_5. N^O = 8-hydroxyquinolinate (hq), M = M′ = Pt, 1; Pd, 2; M = Pt, M′ = Pd, 3) and $[NBu_4][(R_F)_2Pt(\mu\text{-}PPh_2)_2M(N^\wedge O)]$ (R_F = C_6F_5. N^O = picolinate (pic), M = Pt 4; Pd, 5). The synthesis of the asymmetric complexes **1**, **4**, and **5** (Scheme 1a) was carried out by elimination of the bridging chloro ligands as AgCl from the corresponding tetranuclear derivatives $[NBu_4]_2[\{(R_F)_2Pt(\mu\text{-}PPh_2)_2M(\mu\text{-}Cl)\}_2]$,[37] and treatment of the resulting species with the corresponding N^O-donor ligand. Complexes **2** and **3** were obtained by reacting the anion *cis*-$[Pt(R_F)_2(PPh_2)_2]^{2-}$[37] with the binuclear $[\{Pd(\mu\text{-}Cl)(N^\wedge O)\}_2]$ complexes. The anionic moiety behaves as a diphosphane ligand and produces the displacement of the bridging chloro ligand in the binuclear derivative (Scheme 1b). This type of displacement is rather frequent when dinuclear palladium or platinum halido complexes are reacted with bidentate chelating ligands.[35,38−43] The IR spectra of complexes **1**−**5** in the solid state confirmed the presence of the ligands in the respective complexes. These were characterized by elemental analysis, high resolution mass spectrometry, and NMR spectroscopy. The ^{19}F NMR spectra of the complexes were recorded in deuteroacetone, and the relevant data are collected in Experimental Section. In these complexes, the two pentafluorophenyl groups are inequivalent, but the chemical environments of the two rings are very similar and some ^{19}F nuclei were almost isochronous. The $^{31}P\{^1H\}$ NMR spectra are more informative. In all cases, the two inequivalent P atoms appear at high fields (in the range −100 to −145 ppm) as expected for a "$M(\mu\text{-}PPh_2)_2M$" (M = Pt, Pd) fragment without a metal−metal bond.[44−46] As previously noted,[47] the phosphanido ^{31}P NMR signals appear at lower field when Pd atoms were present in the molecule. The assignment of the proper signal to each of the phosphanido P atoms (Table 1) was made on the basis of the $^1H-^{31}P$ HMQC and ^{1}H NOESY spectra. In fact, once assigned the *ortho* protons of the phenyl rings bonded to the P atoms by means of the $^1H-^{31}P$ HMQC, the position of the PPh_2 group was established thanks to the NOE contact between the *ortho* protons of the phenyls and the N−C-*H* protons of the N^O ligand. The attribution of the coupling constants between P and Pt was made by comparison of $^{31}P\{^1H\}$ and $^{195}Pt\{^1H\}$ spectra. The $^{195}Pt\{^1H\}$ spectra of **1**, **3**, **4**, **5** showed broad multiplets at ca. δ −3900 for the Pt^1 atoms bonded to the pentafluorophenyl rings. For **1** and **4**, the $^{195}Pt\{^1H\}$ spectra showed also sharp signals at δ −3450 (**1**) or δ −3542 (**4**) for the Pt^2 atom bonded to the N^O ligand (Table

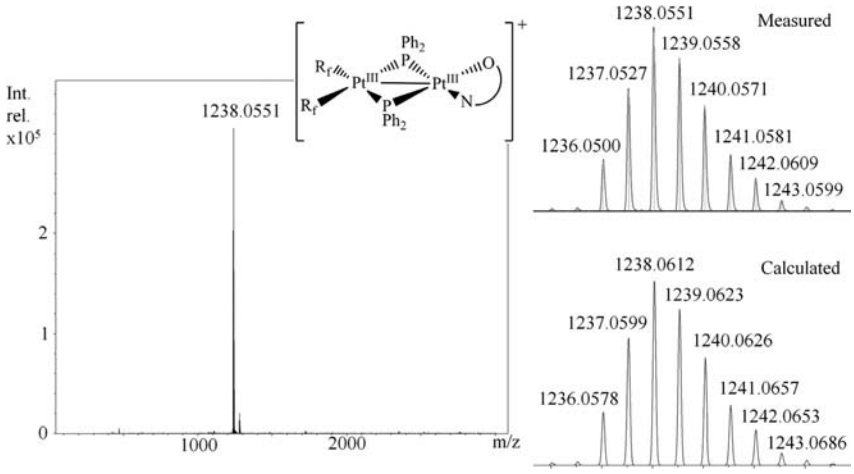

Figure 1. HRMS(+) spectrogram of **1** in MeCN showing the peak corresponding to the cation $[(R_F)_2Pt(\mu\text{-}PPh_2)_2Pt(hq)]^+$. The error between calculated and observed isotopic patterns is 5.3 ppm.

Scheme 2

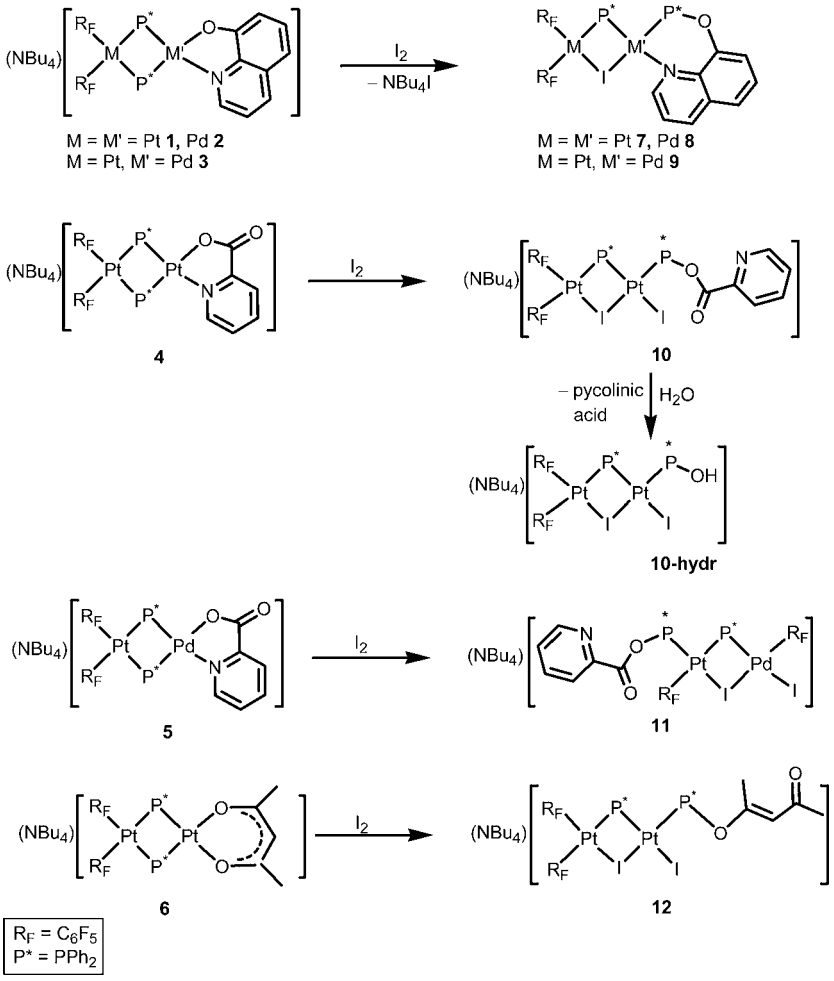

1). The geminal coupling constants between the two Pt atoms in these complexes were 289 and 284 Hz, respectively. The full assignment of all ^{1}H NMR signals was made by means of 1D and 2D ^{1}H NMR spectra and is reported in the Experimental Section.

The HRMS(−) analysis of the anionic complexes **1**−**5** showed the peaks corresponding to their formulas. Given that the electrospray ionization source can act as an electrochemical cell capable to assist redox processes,[48,49] we tested the possibility to oxidize electrochemically the anionic complexes **1**−**5** by submitting them to HRMS(+) analysis in positive mode. In the conditions detailed in the Experimental Section, the five monoanions were smoothly oxidized and the HRMS(+) spectrograms showed intense peaks ascribable to

the corresponding monocationic complexes deriving from loss of two electrons. This suggests that an electrochemical oxidation of **1**−**5** occurs to give probably the corresponding M(III),M′(III) species of the general formula $[(R_F)_2M^{III}(\mu\text{-}PPh_2)_2M'^{III}(L_2)]^+$(Pt−Pt) ($L_2$ = N^O). Figure 1 shows the HRMS(+) spectrogram of **1**, which could be due to the cation $[(R_F)_2Pt^{III}(\mu\text{-}PPh_2)_2Pt^{III}(hq)]^+$(Pt−Pt).[50] The tendency of **1**−**5** to undergo an electrochemical oxidation was found less marked in the case of the mixed metal Pt−Pd complexes **3** and **5**, with respect to **1**, **2**, and **4**, as indicated by the relative intensities of the ion currents due to the oxidized species.[51]

Reaction of $[NBu_4][(R_F)_2M(\mu\text{-}PPh_2)_2M'(L\text{-}L')]$ with I_2. The addition of I_2 to CH_2Cl_2 solutions of complexes $[NBu_4][(R_F)_2M(\mu\text{-}PPh_2)_2M'(L\text{-}L')]$ (L-L′ = hq, **1**−**3**; pic, **4**, **5**; acac, **6**[39]) in a 1:1 molar ratio afforded complexes **7**−**12** with structures depending on the L-L′ ligand and/or the metal cores (Scheme 2). All products **7**−**12** have a common core constituted by a M-P-M′-I four-membered ring and a coordinated Ph_2P-hq, Ph_2P-pic, or Ph_2P-acac ligand (see Chart 2), which are the result of the PPh_2/L-L′ coupling with P−O bond formation (Scheme 2). Complexes **7**−**12** are nonplanar binuclear derivatives endowed with large M···M (M = Pt, Pd) distances as expected for 32 VEC saturated complexes. As we will comment below, the formation of these ligands is the consequence of a reductive coupling induced by I_2 oxidation. The ligand Ph_2P-hq is coordinated to the metal centers in **7**−**9** as chelating, while Ph_2P-pic and Ph_2P-acac act as monodentate (*κ*-*P*) in complexes **10**−**12**, and the binuclear anion contains also a terminal iodide ligand. Complex **10** was very sensitive to moisture and in solution of wet solvents quantitatively hydrolyses to give **10-hydr** (Scheme 2). In addition, the reaction which produces complex **11** is more complicated since migration of one C_6F_5 group from Pt to Pd occurred.

The HRMS(+) spectrograms of the neutral products **7**−**9** showed intense peaks due to $[M + Na]^+$ adducts, while HRMS(−) analysis of **10**−**12** (for which the complexes are anionic) showed peaks due to $[M]^-$.

The molecular structures of **7**, **9**, **11**, and **12** were established by X-ray diffraction studies. Figures 234−5 show molecular drawings of complexes 7 and **9** and of the anionic parts of complexes **11** and **12**, while Tables 234−5 list the most relevant bond distances and angles for the respective complexes. The crystal structures confirm the dinuclear nature of the complexes. In all cases, the core contains the "Pt(*μ*-

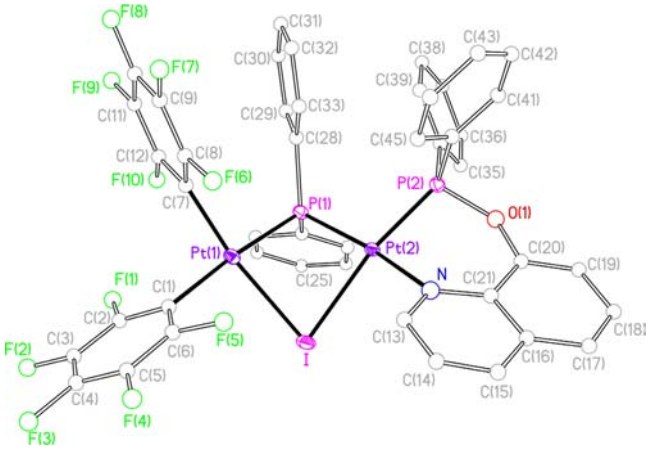

Figure 2. View of the molecular structure of the complex $[(C_6F_5)_2Pt(\mu\text{-}I)(\mu\text{-}PPh_2)Pt(P,N\text{-}Ph_2P\text{-}hq)]$ $2Me_2CO$ (**7**·$2Me_2CO$). Solvent molecules are omitted for clarity.

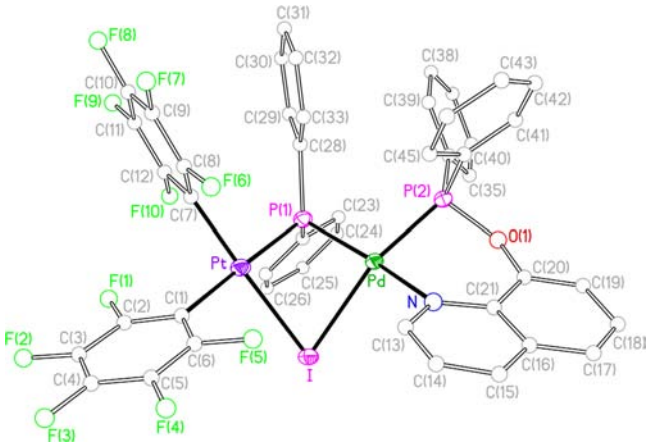

Figure 3. View of the molecular structure of the complex $[(C_6F_5)_2Pt(\mu\text{-}I)(\mu\text{-}PPh_2)Pd(P,N\text{-}Ph_2P\text{-}hq)]$ $Me_2CO\cdot0.25n\text{-}C_6H_{14}$ (**9**·$Me_2CO\cdot0.25n\text{-}C_6H_{14}$). Solvent molecules are omitted for clarity.

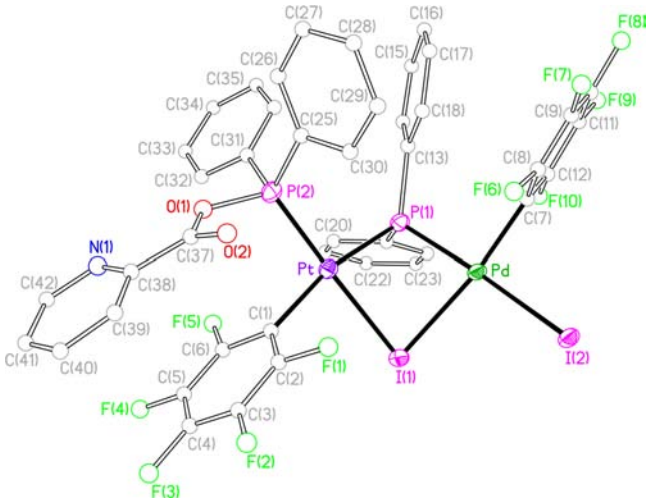

Figure 4. View of the molecular structure of the anion of the complex $[NBu_4][(Ph_2P\text{-}pic)(C_6F_5)Pt(\mu\text{-}I)(\mu\text{-}PPh_2)Pd(C_6F_5)I]$ CH_2Cl_2 (**11**·CH_2Cl_2). Solvent molecules are omitted for clarity.

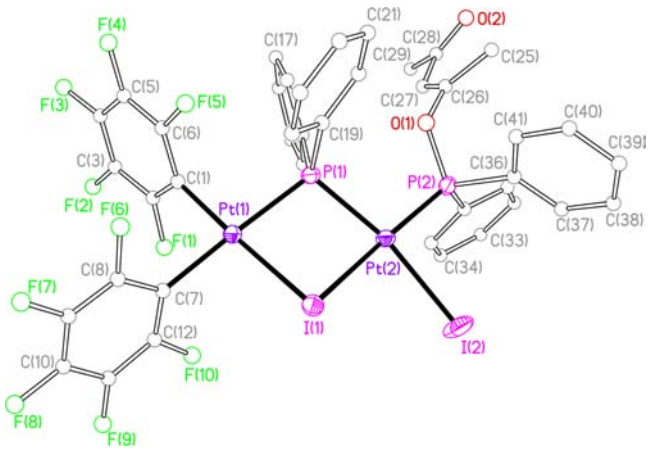

Figure 5. View of the molecular structure of the anion of the complex $[NBu_4][(C_6F_5)_2Pt(\mu\text{-}I)(\mu\text{-}PPh_2)PtI(Ph_2P\text{-}acac)]$ (**12**).

Table 2. Selected Bond Lengths (Å) and Angles (°) for $[(C_6F_5)_2Pt(\mu\text{-}I)(\mu\text{-}PPh_2)Pt(P,N\text{-}PPh_2hq)]\cdot 2Me_2CO$ (7·2Me$_2$CO)

Pt(1)−C(7)	2.005(3)	Pt(1)−C(1)	2.077(3)	Pt(1)−P(1)	2.2853(7)
Pt(1)−I	2.6743(2)	Pt(2)−N	2.149(2)	Pt(2)−P(2)	2.1763(7)
Pt(2)−P(1)	2.2673(7)	Pt(2)−I	2.6971(2)	P(2)−O(1)	1.627(2)
C(7)−Pt(1)−C(1)		90.62(11)	C(7)−Pt(1)−P(1)		94.48(8)
C(1)−Pt(1)−P(1)		174.77(9)	C(7)−Pt(1)−I		169.61(8)
C(1)−Pt(1)−I		93.29(8)	P(1)−Pt(1)−I		81.862(19)
N−Pt(2)−P(2)		86.07(7)	N−Pt(2)−P(1)		166.75(7)
P(2)−Pt(2)−P(1)		102.48(3)	N−Pt(2)−I		92.06(6)
P(2)−Pt(2)−I		167.74(2)	P(1)−Pt(2)−I		81.675(19)
Pt(1)−I−Pt(2)		75.979(6)	Pt(2)−P(1)−Pt(1)		93.14(3)

Table 3. Selected Bond Lengths (Å) and Angles (°) for $[(C_6F_5)_2Pt(\mu\text{-}I)(\mu\text{-}PPh_2)Pd(P,N\text{-}PPh_2hq)]\cdot Me_2CO\cdot 0.25n\text{-}C_6H_{14}$ (9·Me$_2$CO·0.25*n*-C$_6$H$_{14}$)

Pt−C(7)	2.013(3)	Pt−C(1)	2.080(3)	Pt−P(1)	2.2790(9)
Pt−I	2.6788(2)	Pt−Pd	3.1421(3)	Pd−N	2.175(3)
Pd−P(2)	2.2015(8)	Pd−P(1)	2.2641(8)	Pd−I	2.7464(3)
P(2)−O(1)	1.640(2)				
C(7)−Pt−C(1)		88.84(13)	C(7)−Pt−P(1)		92.56(10)
C(1)−Pt−P(1)		178.19(9)	C(7)−Pt−I		177.87(10)
C(1)−Pt−I		93.25(9)	P(1)−Pt−I		85.34(2)
C(7)−Pt−Pd		122.49(10)	C(1)−Pt−Pd		132.15(9)
P(1)−Pt−Pd		46.05(2)	I−Pt−Pd		55.619(6)
N−Pd−P(2)		84.49(7)	N−Pd−P(1)		165.31(8)
P(2)−Pd−P(1)		102.57(3)	N−Pd−I		92.90(7)
P(2)−Pd−I		162.74(2)	P(1)−Pd−I		84.04(2)
N−Pd−Pt		121.07(7)	P(2)−Pd−Pt		141.04(2)
P(1)−Pd−Pt		46.44(2)	I−Pd−Pt		53.608(6)
Pt−I−Pd		70.773(7)	Pd−P(1)−Pt		87.52(3)

Table 4. Selected Bond Lengths (Å) and Angles (°) for $[NBu_4][(PPh_2\text{-pic})(C_6F_5)Pt(\mu\text{-}I)(\mu\text{-}PPh_2)Pd(C_6F_5)I]\cdot CH_2Cl_2$ (11·CH$_2$Cl$_2$)

Pt−C(1)	2.059(4)	Pt−P(2)	2.2074(8)	Pt−P(1)	2.3292(9)
Pt−I(1)	2.6855(2)	Pd−C(7)	2.024(4)	Pd−P(1)	2.2629(8)
Pd−I(2)	2.6807(3)	Pd−I(1)	2.6919(3)	P(2)−O(1)	1.660(3)
C(1)−Pt−P(2)		94.29(10)	C(1)−Pt−P(1)		165.62(10)
P(2)−Pt−P(1)		99.60(3)	C(1)−Pt−I(1)		86.85(9)
P(2)−Pt−I(1)		177.76(2)	P(1)−Pt−I(1)		79.39(2)
C(7)−Pd−P(1)		92.83(10)	C(7)−Pd−I(2)		90.29(10)
P(1)−Pd−I(2)		176.05(3)	C(7)−Pd−I(1)		172.20(11)
P(1)−Pd−I(1)		80.40(2)	I(2)−Pd−I(1)		96.315(10)
Pt−I(1)−Pd		79.463(8)	Pd−P(1)−Pt		96.91(3)

Table 5. Selected Bond Lengths (Å) and Angles (°) for $[NBu_4][(C_6F_5)_2Pt(\mu\text{-}I)(\mu\text{-}PPh_2)PtI(PPh_2\text{-acac})]$ (12)

Pt(1)−C(1)	2.018(7)	Pt(1)−C(7)	2.078(7)	Pt(1)−P(1)	2.308(2)
Pt(1)−I(1)	2.653(1)	Pt(2)−P(1)	2.300(2)	Pt(2)−P(2)	2.198(2)
Pt(2)−I(1)	2.674(1)	Pt(2)−I(2)	2.688(1)	P(2)−O(1)	1.621(5)
C((1)−Pt((1)−C(7)		88.2(3)	C((1)−Pt((1)−P(1)		95.26(19)
C(7)−Pt((1)−P(1)		175.93(18)	C(1)−Pt((1)−I((1)		176.44(17)
C(7)−Pt(1)−I(1)		94.68(18)	P(1)−Pt(1)−I(1)		81.98(5)
P(2)−Pt(2)−P(1)		100.18(7)	P(2)−Pt(2)−I(1)		173.31(5)
P(1)−Pt(2)−I(1)		81.64(5)	P2)−Pt(2)−I(2)		89.53(5)
P(1)−Pt(2)−I(2)		169.51(4)	I(1)−Pt(2)−I(2)		89.17(3)
Pt(1)−I(1)−Pt(2)		85.06(4)	Pt(2)−P(1)−Pt((1)		102.85(7)

PPh$_2$)(μ-I)M" fragment, being M = Pt for **7** and **12**, and M = Pd for **9** and **11**. The intermetallic distances (3.306(1) Å for **7**, 3.142(1) Å for **9**, 3.437(1) Å for **11**, and 3.601(2) Å for **12**) are in agreement with the absence of a M−M bond, as expected for these saturated (32 VEC) complexes. The metal atoms lie in the center of square planes, each plane sharing an edge. The core formed by the two metals and the two bridging atoms is not planar, and the value of the dihedral angle formed by the coordination planes is 53.08(2)° for **7**, 57.52(2)° for **9**, 50.77(2)° for **11**, and 31.93(3)° for **12**. All these structural parameters, along the variability found in the values of the Pt−I−M and Pt−P−M angles, are in agreement with the well-

known flexibility of the "Pt(μ-PPh$_2$)(μ-I)M" central fragment.[33,35,42,52−54]

In complexes **7**, **9** (neutral), and **12** (anionic) the two pentafluorophenyl ligands retain the mutually *cis* disposition to a Pt atom. The other metal atom, Pt(2) in **7**, Pd in **9**, and Pt(2) in **12**, completes its coordination sphere with the formed Ph$_2$P-hq ligand which is coordinated in a *P,N*-chelate mode (complexes **7** and **9**), while in complex **12**, the Ph$_2$P-acac ligand formed in the course of the reaction acts as a monodentate P-donor ligand and the iodide which is present in the mixture completes the coordination environment of Pt(2). Within the acac fragment the sequence of distances C(26)−C(27) 1.337(9), C(27)−C(28) 1.470(9), C(26)−O(1) 1.362(7), and C(28)−O(2) 1.212(8) is different from those of a typical acac ligand,[42,55] as is to be expected according to its rather different bonding situation of this moiety (Chart 2). Finally, in complex **11**, one of the pentafluorophenyl groups has migrated from the Pt to the Pd atom, and the Pt center completes the coordination environment with the P atom of the formed phosphane Ph$_2$P-pic while an iodo ligand completes the coordination sphere of the Pd.

Spectroscopic Properties. The ^{31}P{^{1}H} NMR spectra of **7**−**12** in deuteroacetone solution show the signal due to the P atom of the new phosphinito ligand (Ph$_2$P-hq, Ph$_2$P-pic, Ph$_2$P-acac) at low field (see Table 1), in the 80.6−122.9 δ range. It is well established that in complexes without a metal−metal bond the signal due to the P atom of phosphanido ligand involved in a "M(μ-X)(μ-PPh$_2$)M" fragment (X = halide) appears at lower field than the signals due to the "M(μ-PPh$_2$)$_2$M" fragment.[53,54,56,57] The phosphanido ligands in complexes **7**−**12**, containing a "M(μ-I)(μ-PPh$_2$)M" fragment, appears at lower fields (55.4 to −88.5 ppm) than the starting material, −100.4 to −139.1 ppm. The relationship between δ(μ-P) values and the M-(μ-P)-M angle in bridging phosphanido complexes has long been known.[47] In addition, in complexes **7**, **9**, **11**, and **12** the four atoms M, M′, (μ-I) and (μ-P) are not coplanar in the solid state, and the deviation from the planarity of these four atoms could be related with the dihedral angle α formed by the two planes (μ-P), M, (μ-I) and (μ-P), M′, (μ-I). Noteworthy, in **7**−**12** the δ(μ-^{31}P) range is wide and the δ(μ-^{31}P) values can be related with the structural disposition of the four M, (μ-I), (μ-P), M atoms, i.e., with the planarity of the "M(μ-I)(μ-P)M′" fragment. Table 6 collects data of this α angle for **7**, **9**, **11**, and **12**, as well as for complexes [(R$_F$)$_2$M(μ-I)(μ-PPh$_2$)M′(*P,N*-Ph$_2$P-bzq)] (M, M′ = Pt, **13a**, M = Pt, M′ = Pd, **13b**, M, M′ = Pd, **13c**) reported previously,[34] along with the values of their

Table 6. δ(μ-P) Values (ppm) and Dihedral Angle α (°) in complexes with the fragment "M(μ-P)(μ-I)M′"

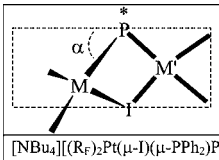	δ(μ-P)	α	Ref.
[NBu$_4$][(R$_F$)$_2$Pt(μ-I)(μ-PPh$_2$)Pt(Ph$_2$P-acac)I], **12**	−90.1	31.93(3)	this work
[NBu$_4$][(R$_F$)(Ph$_2$P-pic)Pt(μ-I)(μ-PPh$_2$)Pd(R$_F$)I], **11**	−47	50.77(2)	this work
[(R$_F$)$_2$Pt(μ-I)(μ-PPh$_2$)Pt(*P,N*-Ph$_2$P-hq)], **7**	−21	53.08(2)	this work
[(R$_F$)$_2$Pt(μ-I)(μ-PPh$_2$)Pt(*P,N*-Ph$_2$P-bzq)], **13a**	−10.9	56	34
[(R$_F$)$_2$Pt(μ-I)(μ-PPh$_2$)Pd(*P,N*-Ph$_2$P-hq)], **9**	48.2	57.52(2)	this work
[(R$_F$)$_2$Pt(μ-I)(μ-PPh$_2$)Pd(*P,N*-Ph$_2$P-bzq)], **13b**	55.6	68	34
[(R$_F$)$_2$Pd(μ-I)(μ-PPh$_2$)Pd(*P,N*-Ph$_2$P-bzq)], **13c**	66.6	68	34

δ(μ-^{31}P). All complexes collected in Table 6 contain the "M(μ-I)(μ-PPh$_2$)M" fragment, and it is apparent that the increase of value of δ(μ-^{31}P) is related to a larger value of α.

The ^{19}F NMR spectra of **7**−**12** in deuteroacetone solution show in all cases two signals due to the *o*-F atoms (2:2 intensity ratio), two signals due to the *m*-F atoms (2:2 intensity ratio), and two signals due to the *p*-F atoms (1:1 intensity ratio). This pattern is in agreement with the presence of two inequivalent C$_6$F$_5$ groups and indicates that the two halves within each C$_6$F$_5$ ring become equivalent in solution. Moreover, *o*- and *m*-F atoms of the R$_F$ rings in *trans* position with respect to P show additional ^{19}F−^{31}P couplings. All data are collected in the Experimental Section. The ^{1}H NMR (1D and 2D) spectra of **7**−**12** show the signals due to the N^O ligands, phenyl groups and the possible counterion (NBu$_4^+$) in the proper intensity ratio. The spectra confirm the stoichiometry of the complexes. The signals due to the N^O-groups in complexes **1**−**5** and those due to the OR part of the phosphinito ligand PPh$_2$OR in **7**−**12** deserve some attention. The signal due to H^2 (see Table 1 for atom numbering) in N^O-chelate shifts significantly downfield when passing from the starting complexes **1**−**5** to the products **7**−**11**. The formation of the P−O bond causes broadening of the ^{1}H signals which experience a (small) P−H coupling, as confirmed by ^{1}H−^{31}P HMQC and ^{1}H{^{31}P} NMR experiments. The ^{1}H NMR spectrum of **12** in deuteroacetone solution shows two signals for the two inequivalent CH$_3$ groups and a signal, a doublet ($^4J_{P,H}$ = 2 Hz), for the C*H* proton of the acac group. The ^{1}H−^{31}P HMQC of **12** showed cross peaks between the phosphinito P and both the C═C−C*H*$_3$ and the C*H* protons.

The ^{195}Pt{^{1}H} spectra of **7** and **9**−**12** showed broad multiplets in the −4020 to −4436 ppm range for the Pt^1 atoms. For **7**, **10**, and **12** the ^{195}Pt{^{1}H} spectra showed also sharp signals at δ −4420 (**7**), δ −3572 (**10**), δ −3500 (**12**) for the Pt^2 atom (Table 1). The geminal coupling constants between the two Pt atoms in these complexes ranged from 1220 to 1283 Hz, values four times higher than those of the respective starting complexes (289 Hz for **1** and 284 Hz for **4**). This effect is presumably due to the substitution of a μ-PPh$_2$ by a μ-I on passing from reagents to products.

Reductive Coupling Between PPh$_2$ and hq, pic, or acac. Considering our previous experience,[33−35,42,54,58] the synthesis of the bimetallic complexes **7**−**12** could, in all likelihood, be the result of an initial oxidation of the diphosphanido dinuclear complexes **1**−**5** by means of I$_2$ in dichloromethane at room temperature, followed by a reductive coupling between one of the bridging PPh$_2$ and the corresponding *O*-donor chelate ligand. The addition of I$_2$ could give either a M(II),M(IV) complex or a binuclear M(III)-M(III) derivative (Chart 1), which would evolve through a P−O reductive coupling to the corresponding Pt(II),Pt(II) final phosphinito complex. In order to gain insights into the mechanism of formation of **7**−**12** and to discriminate between a M(II),M(IV) and a M(III)-M(III) intermediate (Chart 1), we monitored the reaction between **1** and I$_2$ in conditions that hopefully could guarantee the detection of the intermediate. Thus, knowing that for the analogous benzoquinolinate phosphanido M(II),M′(IV) complexes the reductive coupling leading to P^C bond formation was hampered in acetone with the diplatinum species, allowing the isolation of the Pt(II),Pt(IV) intermediate,[34] and given that such Pt(II),Pt(IV) intermediate was quite stable even in dichloromethane in the presence of an excess of iodide, we

monitored the reactions of **1**, **4**, and **6** with I_2 in acetone-d_6 at 268 K, in the presence of 4 equiv of NBu_4I. In these conditions, 3 equiv of iodine were necessary to convert **1** into a new species **1-ox** (>90%), the spectroscopic and spectrometric features of which indicated as the Pt(II),Pt(IV) intermediate depicted in Scheme 3. HRMS-MS/MS and ^{195}Pt NMR data were

Scheme 3. Proposed Pathway for the 1 to 7 Transformation

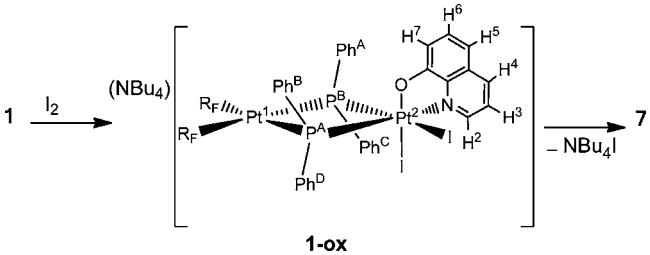

diagnostic for the characterization of **1-ox** as the product of I_2 addition to **1** having a square planar Pt(II) atom bridged by two PPh_2 ligands to an octahedral Pt(IV) atom. In fact, **1-ox** showed at the HRMS(−) analysis an intense peak at m/z 1491.8630 with an isotope pattern superimposable to that of $[\mathbf{1}+2\ I]^-$ (calculated mass = 1491.8712 Da).[59] MS/MS analysis of the peak at m/z 1491.8630 showed fragmentation with loss of I_2, suggesting that the two iodide ligands are in a mutual *cis* position. As to the ^{195}Pt{^{1}H} NMR, we have shown that, for phosphanido complexes, a metal oxidation from +2 to +3 (affording square planar dinuclear species endowed with a Pt(III)−Pt(III) bond) results in a strong ^{195}Pt shielding,[42] whereas metal oxidation from +2 to +4 (affording Pt(II),Pt(IV) dinuclear species) results in a strong ^{195}Pt deshielding.[34]

The ^{195}Pt{^{1}H} spectrum of **1-ox** showed two signals centered at δ −2385 and δ −3774 (Table 7). Of this, the first one is a sharp doublet of doublets (with satellites stemming from the isotopomer having two ^{195}Pt atoms, $^2J_{Pt,Pt}$ = 316 Hz) ascribable to the Pt atom not bonded to the C_6F_5 rings (Pt^2). The deshielding of more than 1000 ppm undergone by Pt^2 on passing from **1** (δ −3450) to **1-ox** (δ −2835) indicates that Pt^2 of **1-ox** is an octahedral Pt(IV). The signal at δ −3774 is a multiplet broadened due to multiple ^{195}Pt−^{19}F couplings and is ascribed to the Pt(II) atom bonded to the C_6F_5 rings (Pt^1), which did not change significantly on passing from **1** (δ_{Pt1} −3903) to **1-ox**.

Complex **1-ox** was characterized in the ^{31}P NMR by two mutually coupled signals at δ −107.5 and δ −84.3, ($^2J_{P,P}$ = 116 Hz). Perusal of multinuclear NMR data indicates that the structure of **1-ox** was that depicted in Scheme 3, with the coordination sites of the octahedral Pt^2(IV) occupied by a iodide and the nitrogen of the hq ligand in the plane containing the two Pt and the two P atoms; the other I and the hq oxygen in the apical positions. Such a structure is analogous to that of **B-ox**, the intermediate formed by addition of I_2 to the benzoquinolinate complex **B** (Chart 1),[34] with the oxygen in place of carbon in the coordination sphere of Pt^2, and for which the XRD structure is known.

The stability of **1-ox** in acetone in the presence of iodide suggests that the mechanism of **1** to **7** transformation (Scheme 3) can be similar to that proposed in our previous work,[34] where a P−C bond formation through reductive coupling between bridging phosphanido and benzoquinolinate groups occurred.[60]

Monitoring in a NMR tube the reaction between **1** and I_2 in acetone-d_6 (in the absence of NBu_4I and with a 1:1 I_2:**1** molar ratio) at 298 K revealed that, immediately after the mixing of the reactants, the mixture contained mainly **1-ox** (plus traces of **1** and **7**) and that, after 48 h, **1-ox** transformed into **7** in ca. 61% spectroscopic yields. The ^{31}P{^{1}H} spectrum of the mixture after 48 h showed also signals ascribable to two species: the tetranuclear Pt(II) complex $[NBu_4]_2[\{(R_F)_2Pt(\mu\text{-}PPh_2)_2Pt(\mu\text{-}I)\}_2]$[35] (ca. 15%) and the iododiphenylphosphane complex $NBu_4[(R_F)_2Pt(\mu\text{-}PPh_2)(\mu\text{-}I)Pt(PPh_2I)I]$ (ca. 21%) featuring signals at δ_P 13.4 ($^2J_{P,P}$ = 10 Hz; $^1J_{Pt,P}$ = 4852 Hz) and δ_P −63.1 ($^2J_{P,P}$ = 10 Hz; $^1J_{Pt,P}$ = 1980 Hz, $^1J_{Pt,P}$ = 2194 Hz). This latter species accounts for the peak at m/z = 1474.7291 (exact mass for the proposed formula = 1474.7306 Da) found in the HRMS(−) spectrogram of the reaction mixture. The MS/MS spectrogram obtained by fragmentation of the m/z = 1474.7291 ion showed only a peak at m/z = 1162.7902 corresponding to the loss of the iododiphenylphosphane.[61] Unfortunately, all attempts to isolate **1-ox** in the state of purity were unsuccessful.

The monitoring at 268 K of the reaction of **4** with I_2 (3 equiv) in the presence of NBu_4I (4 equiv) in acetone-d_6 allowed us to detect, immediately after the mixing of reactants, an intermediate, **4-ox** (Scheme 4), having a structure similar to **1-ox**. The ^{31}P NMR signals of the Pt(II),Pt(IV) complex **4-ox** were found at δ −99.5 (P^A) and δ −77.5 (P^B), while the chemical shift of the octahedral Pt^2(IV) was δ −2501 ppm (Table 7). The HRMS(−) analysis of the solution containing **4-ox** showed an intense signal at m/z = 1469.8500 corresponding to $[\mathbf{4} + 2\ I]^-$ whose fragmentation at the MS/MS analysis consisted of the loss of I_2 with formation of the ion at m/z = 1216.0178. On standing in acetone-d_6 solution at 268 K, **4-ox** slowly reacted to give **10** (after 15 h the mixture contained ca. 35% of **10** and 50% of **4-ox**).[62]

Interestingly, carrying out the monitoring of **4** plus 1 equiv I_2 (without external iodide) in anhydrous thf at 298 K, revealed

Table 7. ^{31}P and ^{195}Pt NMR Data of Intermediates Detected by Monitoring the Reactions of 1, 4, and 6 with I_2 in Deuteroacetone at 268 K[a]

complex	δP^A	δP^B	$^2J_{P^A,P^B}$	$^1J_{P^A,Pt^1}$	$^1J_{P^A,Pt^2}$	$^1J_{P^B,Pt^1}$	$^1J_{P^B,Pt^2}$	δPt^1	δPt^2
B-ox[b]	−115.5	−107.5	126	2032	1807	2189	1270	−3806[c]	−2917[c]
1-ox	−107.5	−84.3	116	2101	1545	2130	1226	−3774[d]	−2385[d]
4-ox	−99.5	−77.5	119	2088	1544	2125	1184	−3810[e]	−2501[e]
10*[g]	−20.4	93.1	15	1906	2257	110	4993	nd	nd
6-ox-*cis*	−73.4	−81.6	102	2126	1641	2140	1260	−3746	−2024[h]
6-ox-*trans*	−88.5			2160	1570			−3746	−2834[i]

[a] δ in ppm, J in Hz. See Schemes 3−5 for numbering. [b] At 298 K, from ref 34. [c] J_{Pt^1,Pt^2} = ca. 100 Hz. [d] $^2J_{Pt^1,Pt^2}$ = 316 Hz. [e] $^2J_{Pt^1,Pt^2}$ = 386 Hz. [g] In thf at 298 K. [h] $^2J_{Pt^1,Pt^2}$ = 225 Hz. [i] $^2J_{Pt^1,Pt^2}$ = 360 Hz

Scheme 4. Proposed Pathway for the 4 to 10 Transformation

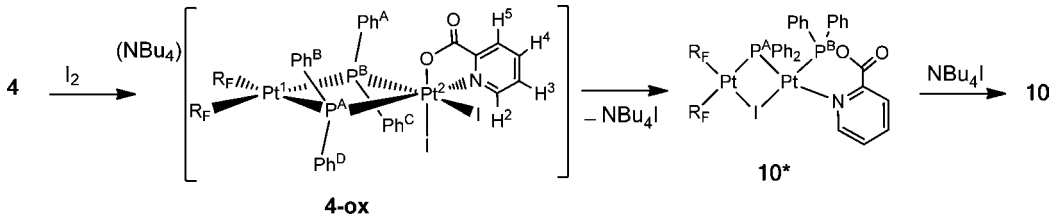

Scheme 5. Proposed Pathway for the 6 to 12 Transformation

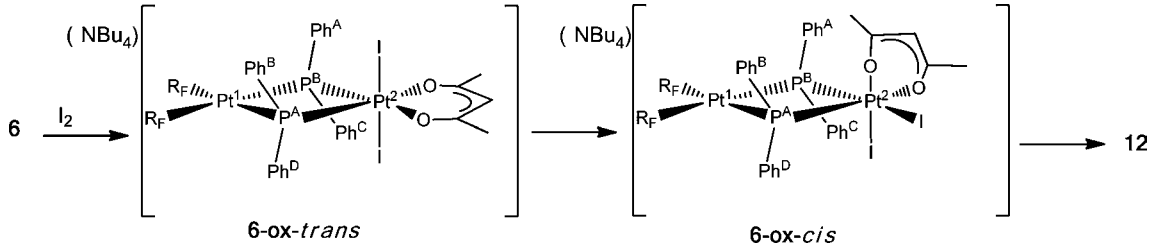

the immediate formation of **4-ox** which progressively transformed into an intermediate, **10***, exhibiting $^{31}P\{^1H\}$ NMR signals at δ_P 93.1 ($^1J_{Pt,P}$ = 4993 Hz) and δ_P −20.4 ($^1J_{Pt,P}$ = 2257 Hz, $^1J_{Pt,P}$ = 1906 Hz) which, in turn, evolved within 1 h into **10**. The similarity of ^{31}P NMR features between **10*** and **7** suggests that the intermediate **10*** might have the structure depicted in Scheme 4, analogous to **7**. The obtainment of **10** as final product from **10*** might therefore be the result of iodide displacement of the coordinated N on Pt^2 (Scheme 4).

Different from the cases of **1** and **4**, the NMR monitoring of the reaction of **6** with 3 equiv of I_2 and in the presence of 4 equiv of NBu_4I at 268 K showed the transformation of **6** into two new species in ca. 60:40 molar ratio. The $^{31}P\{^1H\}$ spectrum of the reaction mixture showed two mutually coupled doublets at δ −73.4 (P^A) and δ −81.6 (P^B), ascribable to a Pt(II),Pt(IV) species, **6-ox**-*cis* (Scheme 5), analogous to **1-ox** (and **4-ox**) along with a singlet at δ −88.5 flanked by two sets of satellites ($J_{P,Pt}$ = 2160 and 1570 Hz). This signal was presumably due to a Pt(II),Pt(IV) species (**6-ox**-*trans*, Scheme 5) having two iodide ligands in mutual *trans* position, in order to justify the symmetry of the molecule evidenced by the NMR data. Accordingly, the $^{195}Pt\{^1H\}$ spectrum of the mixture showed a doublet of doublets at δ −2024 ascribed (by comparison of the P−Pt coupling constants) to the Pt^2(IV) of **6-ox**-*cis*; a triplet at δ −2834 ($J_{P,Pt}$ = 1570 Hz) assigned to the Pt^2(IV) of **6-ox**-*trans*; a broad multiplet at δ −3746 ascribed to the overlapping of the signals due to the Pt^1(II) of **6-ox**-*cis* and **6-ox**-*trans*.

On standing at 268 K, the complex **6-ox**-*trans* quantitatively transformed into **6-ox**-*cis*,[63] which was stable at least for one week in solution at 268 K, allowing us to detect the HRMS(−) signal due to the anion of **6-ox** at m/z = 1446.8716 (calculated mass = 1446.8708 Da). The MS/MS study of the ion at m/z = 1446.8716 showed that it fragmented with a loss of I_2, giving the ion at m/z = 1193.0649.

The Pt(II),Pt(IV) complex **6-ox**-*cis* did not evolve to **12** under these conditions (i.e., deuteroacetone solvent and excess of iodide) even at 298 K. In fact, the $^{31}P\{^1H\}$ spectrum of the reaction mixture recorded after 3 days at 298 K showed only signals of **6-ox**-*cis* along with weak peaks due to $(R_F)_2Pt(\mu\text{-}PPh_2)(\mu\text{-}I)Pt(PPh_2I)I$ and other unidentified species. Carrying out the NMR monitoring of the reaction of **6** with I_2 in acetone-d_6 without external iodide and at 298 K revealed the immediate formation of **6-ox**-*cis* and **6-ox**-*trans* which, within 15 min, rapidly evolved to **12**.

With all this information the synthesis of complexes **7**−**12** could be understood through a similar process observed earlier[34] for the benzoquinolinate derivatives: addition of I_2 to **1**−**6** derivatives gives a dinuclear intermediate with both diphenylphosphanido groups bridging two metal centers, one of them in oxidation state II and the other one in oxidation state IV. The dissociation of a I^- group gives an unsaturated oxidized metal from which the coupling between a bridging PPh_2 and the O-donor ligand forms the new ligand with P−O bond formation. Taking into account that we have isolated the Pt(II),Pt(IV) intermediate $[NBu_4][(R_F)_2Pt^{II}(\mu\text{-}PPh_2)_2Pt^{IV}(C\text{^}N)I_2]$[34] (**B-ox**) and all attempts to achieve pure samples of the Pt(II),Pt(IV) intermediates, **1-ox** and **4-ox**, were unsuccessful, the processes forming Ph_2P-L ligand seem to be easier for Ph_2P-hq, Ph_2P-pic, and Ph_2P-acac (formation of P−O bond) than for Ph_2P-bzq (formation of P−C bond). It is to note that the oxidized intermediates have been detected only for platinum complex, and it is in agreement with the fact that M(IV)-iodo derivatives are usual for platinum but scarce for palladium derivatives.[13,64−66] The processes described here imply a M−P and M−O bond cleavage and a P−O bond formation and result in a formation of $PPh_2(O\text{^}N)$ or $PPh_2(O\text{^}O)$ (Chart 2) from a bridging phosphanido complex and can be considered as an intermediate step for the transition metal-mediated P−C/O exchange at bound phosphane ligands.[67]

Although complexes **7**−**12** can be isolated as pure solids, the coupling between the PPh_2 group and the O-donor ligand is not the only process which takes place in the reaction. The study shows that unidentified species, formed from side reactions, are present and that the iododiphenylphosphane complex $NBu_4[(R_F)_2Pt(\mu\text{-}PPh_2)(\mu\text{-}I)Pt(PPh_2I)I]$ and the tetranuclear derivatives of platinum or palladium(II) $[NBu_4]_2[\{(R_F)_2Pt(\mu\text{-}PPh_2)_2M(\mu\text{-}I)\}_2]$,[35] which could be the result of other type of reductive coupling of ligands, are identified in solution in some of the processes. The iododiphenylphosphane complex might derive from the P−I reductive coupling on the M(II),M(IV) intermediates. The $[NBu_4]_2[\{(R_F)_2Pt(\mu\text{-}PPh_2)_2M(\mu\text{-}I)\}_2]$ complexes[35] show two

dx.doi.org/10.1021/ic4004005 | Inorg. Chem. 2013, 52, 5493−5506

"$(R_F)_2Pt^{II}(\mu\text{-}PPh_2)_2M^{II}$" fragments joined by two I^- groups, i.e., after addition of I_2, the phosphanido groups are still acting as bridging ligands maintaining the polynuclear fragment and behaving as a spectator. The evolution of high oxidation state complexes of palladium and platinum through several paths of reductive coupling is not surprising, and even on phosphanido derivatives we observed the formation of a mixture of products resulting of the P−C and P−P reductive couplings on trinuclear phosphanido complex.[58]

■ CONCLUSIONS

The bridging phosphanido ligand, in anionic derivatives of palladium and platinum(II), is not only used as a way for maintaining the molecular architecture. The transformation of bridging phosphanido ligands into phosphane is now well established.[33−35,42,54,68−72] The addition of I_2 to anionic phosphanido derivatives of palladium and platinum(II) with *O*-donor ligands facilitated the formation of P−O bonds resulting in the phosphane ligands Ph_2P-hq, in complexes **7**−**9**, Ph_2P-pic, in complexes **10** and **11**, and Ph_2P-acac in complex **12**. The process takes place through the intermediate M(II),M(IV) complexes which evolve to undergo easy reductive coupling reactions. In no case was observed the formation of $PPh_2C_6F_5$ from the starting anionic complexes. The oxidation of these diphenylphosphanido complexes allows the identification of intermediates, in some cases stable enough to be isolated and fully characterized, in formal oxidation states Pt(III)(square-planar)-Pt(III)(square-planar) or Pt(II)(square-planar)-Pt(IV)(octahedral). Both type of complexes seem to be not too different, and in fact the formation of the Pt(II),Pt(IV) derivatives can be considered as formed by the addition of two I^- ligands to the same metal center of the dinuclear Pt(III)−Pt(III) compounds. The high oxidation state intermediates observed in the described reactions could provide opportunities for achieving distinct and complementary reactivity of the phosphanido complexes. This reactivity paves the way for the synthesis of specific ligands through two steps: (a) synthesis of the adequate starting material by a formal coordination of a chelate L-L′ ligand (*O*-donor group) to the "$(R_F)_2Pt^{II}(\mu\text{-}PPh_2)_2M^{II}$" fragment and (b) oxidation of this new phosphanido complex which induces the formation of a P−L bond providing the designed new ligand Ph_2P-LL′.

■ EXPERIMENTAL SECTION

General Comments. C, H, and N analyses were performed with a Perkin-Elmer 2400 analyzer. IR spectra were recorded on a Perkin-Elmer Spectrum 100 FT-IR spectrometer. NMR spectra in solution were recorded on Bruker Avance 400 spectrometers with $SiMe_4$, $CFCl_3$, 85% H_3PO_4, and aqueous $[PtCl_6]^{2-}$ as external references for ^1H, ^{19}F, ^{31}P, and ^{195}Pt, respectively. High resolution mass spectrometry (HRMS) and MS/MS analyses were performed using a time-of-flight mass spectrometer equipped with an electrospray ion source (Bruker micrOTOF-Q II). The analyses were carried out in positive and in negative ion modes. The samples were introduced as acetonitrile solutions by continuous infusion with the aid of a syringe pump at a flow-rate of 180 μL/h. The instrument was operated at end plate offset −500 V and capillary −4500 V. Nebulizer pressure was 0.3 bar (N_2) and the drying gas (N_2) flow 4 L/min. Drying gas temperature was set at 453 K. The software used for the simulations is Bruker Daltonics Data Analysis (version 4.0). For all described HRMS peaks, the isotope patterns were superimposable to those calculated on the basis of the proposed formulas. Literature methods were used to prepare the starting materials *cis*-$[M(R_F)_2(PPh_2H)_2]$ (M = Pd, Pt),[37] $[NBu_4]_2[\{(R_F)_2Pt(\mu\text{-}PPh_2)_2M(\mu\text{-}Cl)\}_2]$ (M = Pd, Pt),[37] $[\{Pd(\mu\text{-}Cl)(hq)\}_2]$,[73] $[NBu_4][(R_F)_2Pt(\mu\text{-}PPh_2)_2Pt(acac)]$ (**6**).[39]

Synthesis of $[NBu_4][(R_F)_2M(\mu\text{-}PPh_2)_2M'(hq)]$. *M = M′ = Pt,* ***1***. $AgClO_4$ (0.118 g, 0.570 mmol) was added to a colorless solution of $[NBu_4]_2[\{(R_F)_2Pt(\mu\text{-}PPh_2)_2Pt(\mu\text{-}Cl)\}_2]$ (0.783 g, 0.285 mmol) in acetone (25 mL). The mixture was stirred in the dark for 1 h. 8-Hydroxyquinoline (0.083 g, 0.570 mmol) was added and stirred for 30 min. NBu_4OH (1 M in methanol, 0.6 mL, 0.6 mmol) was added, and after 30 min the mixture was filtered through Celite. The yellow solution was evaporated to ca. 2 mL and *i*-PrOH (ca. 15 mL) was added. Complex **1** crystallized as a yellow solid which was filtered, washed with cold *i*-PrOH (3 × 1 mL), and dried. Yield: 0.553 g, 65%. Found: C, 49.59; H, 4.47; N, 1.82. $C_{61}H_{62}F_{10}N_2OP_2Pt_2$ requires C, 49.46; H, 4.22; N, 1.89. HRMS(−), exact mass for the anion $[C_{45}H_{26}F_{10}NOP_2Pt_2]^-$: 1238.0622; measured: *m/z*: 1238.0623 $(M)^-$. ^1H NMR (298 K, $(CD_3)_2CO$, 400 MHz): δ 8.33 (d, 1H, H^4, 8.4 Hz), 8.12 (broad, 1H, H^2), 8.00 (dd, 4H, *o*-Ph bonded to P^A, 10.5 Hz, 7.6 Hz), 7.92 (pseudo t, 4H, *o*-Ph bonded to P^B, 9.1 Hz), 7.41 (pseudo t, 1H, H^6, 7.4 Hz), 7.28−7.13 (m, 13 H, overlapped H^3, *m*-Ph, *p*-Ph), 6.88 (d, 1H, H^5, 7.9 Hz), 6.82 (d, 1H, H^7, 7.9 Hz), 3.49 (m, 8H, NBu_4^+), 1.87 (m, 8H, NBu_4^+), 1.49 (pseudo sextet, 8H, 7.4 Hz, NBu_4^+), 1.03 (t, 12H, 7.4 Hz, NBu_4^+) ppm. ^{19}F NMR (298 K, $(CD_3)_2CO$, 376.5 MHz): δ −114.8 (m, 4 *o*-F, $^3J_{F,Pt}$ = ca. 330 Hz), −168.3 (m, 4 *m*-F), −167.3 (m, 2 *p*-F).

M = M′ = Pd, ***2***. *n*-Butyllitium (2.5 M in hexanes, 0.50 mL, 1.25 mmol) was added to a colorless solution of *cis*-$[Pd(C_6F_5)_2(PPh_2H)_2]$ (0.500 g, 0.615 mmol) in thf (15 mL) under an argon atmosphere at −78 °C. The yellow solution was stirred for 15 min and $[\{Pd(\mu\text{-}Cl)(8\text{-}hq)\}_2]$ (0.176 g, 0.308 mmol) was added. The suspension was allowed to reach room temperature, stirred for 20 h, and evaporated to dryness. CH_2Cl_2 (25 mL) was added to the resulting residue, and a solid was filtered through Celite. The CH_2Cl_2 solution was evaporated to dryness, and the residue was dissolved in *i*-PrOH (ca. 35 mL). NBu_4ClO_4 (0.212 g, 0.617 mmol) was added to the solution and **2** started to crystallize. The solution was evaporated to ca. 20 mL and left in the freezer for 4 h. **2** crystallized as a yellow solid, which was filtered, washed with cold *i*-PrOH (3 × 1 mL), and dried, 0.362 g, 45% yield. Found: C, 56.59; H, 4.73; N, 2.13. $C_{61}H_{62}F_{10}N_2OP_2Pd_2$ requires C, 56.19; H, 4.79; N, 2.15. HRMS(−), exact mass for the anion $[C_{45}H_{26}F_{10}NOP_2Pd_2]^-$: 1061.9399; measured: *m/z*: 1061.9428 $(M)^-$. ^1H NMR (298 K, $(CD_3)_2CO$, 400 MHz): δ 8.20 (d, 1H, H^4, 8.3 Hz), 7.99 (dd, 4H, *o*-Ph bonded to P^A, 10.4 Hz, 7.7 Hz), 7.91 (dd, 4H, *o*-Ph bonded to P^B, 10.1 Hz, 7.8 Hz), 7.63 (broad, 1H, H^2), 7.32 (pseudo t, 1H, H^6, 8.1 Hz), 7.25 (t, 2H, *p*-Ph bonded to P^B, 6.7 Hz), 7.23 (t, 2H, *p*-Ph bonded to P^A, 6.7 Hz), 7.18 (t, 4H, *m*-Ph bonded to P^B, 7.4 Hz), 7.12 (t, 4H, *m*-Ph bonded to P^A, 7.2 Hz), 7.07 (dd, 1H, H^3, 7.9 Hz, 4.8 Hz), 6.81 (d, 1H, H^5, 7.9 Hz), 6.72 (d, 1H, H^7, 7.9 Hz), 3.49 (m, 8H, NBu_4^+), 1.87 (m, 8H, NBu_4^+), 1.49 (pseudo sextet, 8H, 7.4 Hz, NBu_4^+), 1.03 (t, 12H, 7.4 Hz, NBu_4^+) ppm. ^{19}F NMR (298 K, $(CD_3)_2CO$, 376.5 MHz): δ −111.5 (m, 2 *o*-F), −111.7 (2 *o*-F), −167.0 (m, 4 *m*-F), −166.2 (m, 1 *p*-F), −166.3 (m, 1 *p*-F).

M = Pt, M′ = Pd, ***3***. Complex **3** was prepared similarly to **2** from *cis*-$[Pt(C_6F_5)_2(PPh_2H)_2]$ (0.610 g, 0.676 mmol), *n*-butyllitium (2.5 M in hexane, 0.54 mL, 1.35 mmol), $[\{Pd(\mu\text{-}Cl)(8\text{-}hq)\}_2]$ (0.193 g, 0.337 mmol) and NBu_4ClO_4 (0.231 g, 0.676 mmol) as a yellow solid. 0.478 g, 51% yield. Found: C, 52.70; H, 4.43; N, 1.96. $C_{61}H_{62}F_{10}N_2OP_2PdPt$ requires C, 52.61; H, 4.49; N, 2.01. HRMS(−), exact mass for the anion $[C_{45}H_{26}F_{10}NOP_2PdPt]^-$: 1150.0005; measured: *m/z*: 1149.9899 $(M)^-$. ^1H NMR (298 K, $(CD_3)_2CO$, 400 MHz): δ 8.21 (d, 1H, H^4, 8.3 Hz), 8.01 (pseudo t, 4H, *o*-Ph bonded to P^A, 8.8 Hz), 7.92 (dd, 4H, *o*-Ph bonded to P^B, 9.1 Hz), 7.70 (broad, 1H, H^2), 7.32 (pseudo t, 1H, H^6, 8.0 Hz), 7.29−7.08 (m, 13 H, overlapped H^3, *m*-Ph, *p*-Ph), 6.82 (d, 1H, H^5, 7.9 Hz), 6.73 (d, 1H, H^7, 7.9 Hz), 3.49 (m, 8H, NBu_4^+), 1.87 (m, 8H, NBu_4^+), 1.49 (pseudo sextet, 8H, 7.4 Hz, NBu_4^+), 1.03 (t, 12H, 7.4 Hz, NBu_4^+) ppm. ^{19}F NMR (298 K, $(CD_3)_2CO$, 376.5 MHz): δ −114.7 (m, 2 *o*-F, $^3J_{F,Pt}$ = 324 Hz), −115.0 (m, 2 *o*-F, $^3J_{F,Pt}$ = 330 Hz), −168.1 (m, 4 *m*-F), −167.3 (m, 2 *p*-F) ppm.

Synthesis of $[NBu_4][(R_F)_2Pt(\mu\text{-}PPh_2)_2M(pic)]$. *M = Pt,* ***4***. Complex **4** was prepared similarly to **1** from $[NBu_4]_2[\{(R_F)_2Pt(\mu\text{-}PPh_2)_2Pt(\mu\text{-}Cl)\}_2]$ (0.362 g, 0.132 mmol), $AgClO_4$ (0.055 g, 0.264 mmol), picolinic acid (0.032 g, 0.264 mmol), and NBu_4OH (1 M in methanol, 0.3 mL, 0.300 mmol) as a white solid. Yield: 0.217 g, 57%.

Found: C, 47.34; H, 3.61; N 1.90. $C_{58}H_{60}F_{10}N_2P_2Pt_2$ requires C, 47.74; H, 4.14; N, 1.92. HRMS(−), exact mass for the anion $[C_{42}H_{24}F_{10}NO_2P_2Pt_2]^-$: 1216.0415; measured: *m/z*: 1216.0350 (M)$^-$. ^{1}H NMR (298 K, $(CD_3)_2CO$, 400 MHz): δ 8.16 (pseudo td, 1H, H^4, 7.5 Hz, 1.3 Hz), 8.08 (d, 1H, H^5, 7.5 Hz), 8.02 (d, 1H, H^2, 5.0 Hz), 7.90 (pseudo t, 4H, *o*-Ph bonded to P^A, 8.8 Hz), 7.88 (pseudo t, 4H, *o*-Ph bonded to P^B, 8.8 Hz), 7.47 (dd, 1H, H^2, 7.5 Hz, 5.9 Hz), 7.32−7.15 (m, 12 H, *m*-Ph, *p*-Ph), 3.49 (m, 8H, NBu_4^+), 1.87 (m, 8H, NBu_4^+), 1.49 (pseudo sextet, 8H, 7.4 Hz, NBu_4^+), 1.03 (t, 12H, 7.4 Hz, NBu_4^+) ppm. ^{19}F NMR (298 K, $(CD_3)_2CO$, 376.5 MHz): δ −115.0 (m, 2 *o*-F, $^3J_{F,Pt}$ = 323 Hz), −115.1 (m, 2 *o*-F, $^3J_{F,Pt}$ = 325 Hz), −168.0 (m, 4 *m*-F), −167.2 (m, 2 *p*-F) ppm.

M = Pd, ***5***. Complex **5** was prepared similarly to **1** from $[NBu_4]_2[\{(R_F)_2Pt(\mu\text{-}PPh_2)_2Pd(\mu\text{-}Cl)\}_2]$ (0.200 g, 0.078 mmol), $AgClO_4$ (0.032 g, 0.156 mmol), picolinic acid (0.019 g, 0.156 mmol), and NBu_4OH (1 M in methanol, 0.16 mL, 0.160 mmol) as a yellow solid 0.135 g, 63% yield. Found: C, 50.72; H, 4.26; N, 2.26. $C_{58}H_{60}F_{10}N_2P_2Pt_2PdPt$ requires C, 50.83; H, 4.41; N, 2.04. HRMS(−), exact mass for the anion $[C_{42}H_{24}F_{10}NO_2P_2PtPd]^-$: 1127.9787; measured: *m/z*: 1127.9741 (M)$^-$. ^{1}H NMR (298 K, $(CD_3)_2CO$, 400 MHz): δ 8.10 (d, 1H, H^5, 7.6 Hz), δ 8.04 (pseudo t, 1H, H^4, 7.6 Hz), 7.93 (m, 4H, *o*-Ph bonded to P^A, overlapped), 7.89 (m, 4H, *o*-Ph bonded to P^B, overlapped), 7.64 (d, 1H, H^2, 4.1 Hz), 7.37−7.14 (m, 13 H, *m*-Ph, *p*-Ph, H^3), 3.49 (m, 8H, NBu_4^+), 1.87 (m, 8H, NBu_4^+), 1.49 (pseudo sextet, 8H, 7.4 Hz, NBu_4^+), 1.03 (t, 12H, 7.4 Hz, NBu_4^+) ppm. ^{19}F NMR (298 K, $(CD_3)_2CO$, 376.5 MHz): δ −115.0 (m, 2 *o*-F, $^3J_{F,Pt}$ = ca. 325 Hz), −115.1 (m, 2 *o*-F, $^3J_{F,Pt}$ = ca. 335 Hz), −167.1 (m, 4 *m*-F), −167.7 (m, 1 *p*-F), −167.8 (m, 1 *p*-F) ppm.

Synthesis of $[(R_F)_2M(\mu\text{-}I)(\mu\text{-}PPh_2)M'(P,O\text{-}PPh_2hq)]$. *M = M′ = Pt,* ***7***. I_2 (0.029 g, 0.114 mmol) in CH_2Cl_2 (10 mL) was added dropwise to a yellow solution of **1** (0.169 g, 0.114 mmol) in CH_2Cl_2 (5 mL). The solution was stirred at room temperature for 20 h, and the orange solution was evaporated to ca. 1 mL. *i*-PrOH (10 mL) was added, stirred for 30 min, and left in the freezer for 4 h. Complex **7** crystallized as a yellow solid which was filtered, washed with cold *i*-PrOH (2 × 1 mL), and dried. Yield: 0.098 g, 63%. Found: C, 39.27; H, 1.96; N, 1.16. $C_{45}H_{26}F_{10}INOP_2Pt_2$ requires C, 39.58; H, 1.92; N, 1.03. HRMS(+), measured: *m/z*: 1387.9561 [M + Na]$^+$, exact mass: 1387.9554; ^{1}H NMR (298 K, $(CD_3)_2CO$, 400 MHz): δ 10.53 (broad d, 1H, H^2, 4.9 Hz), 8.97 (d, 1H, H^4, 8.4 Hz), 8.05 (d, 1H, H^5, 8.0 Hz, overlapped), 8.03 (m, 1H, H^3, overlapped), 7.88 (d, 1H, H^7, 8.0 Hz), 7.81 (pseudo t, 1H, H^6, 8.0 Hz), 7.65−7.52 (m, 6H, *o*-Ph bonded to P^B, *p*-Ph bonded to P^B), 7.46−7.34 (m, 8H, *o*-Ph bonded to P^A, *m*-Ph bonded to P^B), 7.27 (t, 2H, *p*-Ph bonded to P^A, 7.5 Hz), 7.09 (pseudo t, 4H, *m*-Ph bonded to P^A, 7.5 Hz) ppm. ^{19}F NMR (298 K, $(CD_3)_2CO$, 376.5 MHz): δ −115.4 (m, 2 *o*-F of the R_F *trans* to P, $^3J_{F,Pt}$ = 336 Hz, $^3J_{F,F}$ = $^3J_{F,P}$ = 18 Hz), −117.5 (d, 2 *o*-F of the R_F *trans* to I, $^3J_{F,Pt}$ = 528 Hz, $^3J_{F,F}$ = 27 Hz), −165.1 (t, 1 *p*-F of the R_F *trans* to P, $^3J_{F,F}$ = 19 Hz), −166.1 (td, 2 *m*-F of the R_F *trans* to P, $^3J_{F,F}$ = 19 Hz, $^5J_{F,P}$ = 9 Hz), −167.2 (t, 1 *p*-F of the R_F *trans* to I, $^3J_{F,F}$ = 19 Hz), −167.5 (m, 2 *m*-F of the R_F *trans* to I, $^4J_{F,Pt}$ = 130 Hz, $^3J_{F,F}$ = 19 Hz, $^3J_{F,F}$ = 27 Hz) ppm.

M = M′ = Pd, ***8***. I_2 (0.039 g, 0.157 mmol) in CH_2Cl_2 (10 mL) was added dropwise to a yellow solution of **2** (0.204 g, 0.157 mmol) in CH_2Cl_2 (5 mL), and the resulting mixture was stirred at room temperature for 20 h. The red solution was evaporated to ca. 1 mL, passed through a silica column (ca. 15 cm ×3 cm^2) and eluted with CH_2Cl_2. The red solution (ca. 50 mL) was evaporated to ca. 1 mL, Et_2O (30 mL), and hexane (ca. 2 mL) was added and left in the freezer for 4 h. A red solid, **8**, was filtered, washed with cold *n*-hexane (2 × 1 mL), and dried. 0.040 g, 21% yield. Solutions of **8** slowly became dark. Minor amounts of black palladium could be present in the samples of **8**. Found: C, 44.34; H, 2.40; N, 1.18. $C_{45}H_{26}F_{10}INOP_2Pd_2$ requires C, 45.48; H, 2.21; N, 1.18. HRMS(+), measured: *m/z*: 1211.8283 [M + Na]$^+$, exact mass: 1211.8359; ^{1}H NMR (298 K, $(CD_3)_2CO$, 400 MHz): δ 10.46 (broad d, 1H, H^2, 4.9 Hz), 8.88 (dd, 1H, H^4, 8.3 Hz, 1.4 Hz), 8.00 (dd, 1H, H^3, 8.3 Hz, 5.0 Hz), 7.98 (d, 1H, H^5, 8.0 Hz, 1.4 Hz), 7.82 (ddd, 1H, H^7, 7.7 Hz, 1.3 Hz, 0.7 Hz), 7.75 (pseudo t, 1H, H^6, 8.0 Hz), 7.64 (t, 2H, *p*-Ph bonded to P^B, 7.3 Hz), 7.54 (dd, 4H, *o*-Ph bonded to P^B, 12.4 Hz, 8.2 Hz) 7.44 (ddd, 4H, *m*-Ph bonded to P^B, 8.2 Hz, 7.3 Hz, 3.4 Hz), 7.36−7.29 (m, 6H, *p*-Ph bonded to P^A, *o*-Ph bonded to P^A), 7.11 (ddd, 4H, *m*-Ph bonded to P^A, 8.0 Hz, 7.5 Hz, 2.2 Hz) ppm. ^{19}F NMR (298 K, $(CD_3)_2CO$, 376.5 MHz): δ −112.6 (m, 2 *o*-F of the R_F *trans* to P, $^3J_{F,F}$ = 31 Hz), −113.8 (m, 2 *o*-F of the R_F *trans* to I, $^3J_{F,F}$ = 24 Hz), −164.2 (t, 1 *p*-F of the R_F *trans* to P, $^3J_{F,F}$ = 19 Hz), −165.1 (td, 1 *p*-F of the R_F *trans* to I, $^3J_{F,F}$ = 19 Hz, $^4J_{F,F}$ = 2 Hz), −165.3 (ddd, 2 *m*-F of the R_F *trans* to P, $^3J_{F,F}$ = 31 Hz, $^3J_{F,F}$ = 19 Hz, $^5J_{F,P}$ = 11 Hz), −165.9 (dd, 1 *m*-F of the R_F *trans* to I, $^3J_{F,F}$ = 24 Hz, $^3J_{F,F}$ = 19 Hz) ppm.

M = Pt, M′ = Pd, ***9***. Complex **9** was prepared similarly to **8** from **3** (0.203 g, 0.145 mmol) and I_2 (0.037 g, 0.145 mmol) as a orange solid. 0.052 g, 28% yield. Found: C, 42.14; H, 2.24; N, 1.34 $C_{45}H_{26}F_{10}INOP_2PdPt$ requires C, 42.32; H, 2.05; N, 1.10. HRMS(+), measured: *m/z*: 1299.8893 [M + Na]$^+$, exact mass: 1299.8937; ^{1}H NMR (298 K, $(CD_3)_2CO$, 400 MHz): δ 10.49 (broad d, 1H, H^2, 4.3 Hz), 8.89 (d, 1H, H^4, 8.3 Hz), 8.03−7.96 (m, 2H, H^3 + H^5), 7.82 (d, 1H, H^7, 7.3 Hz), 7.75 (pseudo t, 1H, H^6, 7.7 Hz), 7.66 (t, 2H, *p*-Ph bonded to P^B, 7.1 Hz), 7.57−7.43 (m, 8H, *o*-Ph bonded to P^B, *m*-Ph bonded to P^B), 7.36−7.26 (m, 6H, *p*-Ph bonded to P^A, *o*-Ph bonded to P^A), 7.11 (pseudo t, 4H, *m*-Ph bonded to P^A, 7.3 Hz) ppm. ^{19}F NMR (298 K, $(CD_3)_2CO$, 376.5 MHz): δ −115.8 (m, 2 *o*-F of the R_F *trans* to P, $^3J_{F,Pt}$ = 336 Hz, $^3J_{F,F}$ = $^3J_{F,P}$ = 18 Hz), −117.9 (d, 2 *o*-F of the R_F *trans* to I, $^3J_{F,Pt}$ = 515 Hz, $^3J_{F,F}$ = 27 Hz), −164.9 (t, 1 *p*-F of the R_F *trans* to P, $^3J_{F,F}$ = 20 Hz), −166.1 (td, 2 *m*-F of the R_F *trans* to P, $^3J_{F,F}$ = 20 Hz, $^5J_{F,P}$ = 9 Hz), −166.7 (t, 1 *p*-F of the R_F *trans* to I, $^3J_{F,F}$ = 19 Hz), −167.2 (m, 2 *m*-F of the R_F *trans* to I, $^4J_{F,Pt}$ = 168 Hz, $^3J_{F,F}$ = 19 Hz, $^3J_{F,F}$ = 27 Hz) ppm.

Reaction of ***4*** *with* I_2. I_2 (0.030 g, 0.118 mmol) was added to a yellow solution of **4** (0.173 g, 0.118 mmol) in anhydrous CH_2Cl_2 (10 mL), and the resulting mixture was stirred under argon at room temperature for 20 h. The resulting solution was evaporated to ca. 3 mL, anhydrous *n*-hexane (10 mL) was added, and a yellow oil was formed. The liquors were eliminated, and the yellow oil was stirred with anhydrous *n*-hexane (5 mL) for 30 min affording a yellow solid. The *n*-hexane was eliminated, and the solid was dried in a vacuum. The ^{31}P{^{1}H}NMR spectrum of this yellow solid showed to be a mixture of $[NBu_4][(R_F)_2Pt(\mu\text{-}I)(\mu\text{-}PPh_2)Pt(PPh_2\text{-pic})I]$, **10**, and $[NBu_4][(R_F)_2Pt(\mu\text{-}I)(\mu\text{-}PPh_2)Pt(PPh_2OH)I]$, **10-hydr**, and satisfactory analysis of **10** could in no case be obtained. Recrystallization of this mixture from wet acetone and *i*-PrOH (1 mL/5 mL) afforded **10-hydr** which was filtered, washed with cold *i*-PrOH (2 × 0.5 mL), and dried. **10-hydr**. Yield: 0.111 g, 54%. Found: C, 38.81; H, 3.31; N, 0.98. $C_{52}H_{57}F_{10}I_2NOP_2Pt_2$ requires C, 38.84; H, 3.57; N, 0.87.

10. HRMS(−), exact mass for the anion $[C_{42}H_{24}F_{10}NI_2O_2P_2Pt_2]^-$: 1469.8504 Da; measured: *m/z*: 1469.8517 (M)$^-$. ^{1}H NMR (298 K, $(CD_3)_2CO$, 400 MHz): δ 8.62 (broad d, 1H, H^2, 4.3 Hz), 8.01 (dd, 4H, *o*-Ph bonded to P^B, 7.1 Hz, 8.5 Hz), 7.84−7.77 (m, 5H, *o*-Ph bonded to P^A, H^4), 7.58−7.39 (m, 8H, *p*-Ph bonded to P^B, *m*-Ph bonded to P^B, H^3, H^5), 7.10 (t, 2H, *p*-Ph bonded to P^A, 6.9 Hz), 7.00 (pseudo t, 4H, *m*-Ph bonded to P^A, 7.3 Hz), 3.49 (m, 8H, NBu_4^+), 1.87 (m, 8H, NBu_4^+), 1.49 (pseudo sextet, 8H, 7.4 Hz, NBu_4^+), 1.03 (t, 12H, 7.4 Hz, NBu_4^+) ppm. ^{19}F NMR (298 K, $(CD_3)_2CO$, 376.5 MHz): δ −114.9 (pseudo t, 2 *o*-F of the R_F *trans* to P, $^3J_{F,Pt}$ = 340 Hz, $^3J_{F,F}$ = $^3J_{F,P}$ = 19 Hz), −116.4 (d, 2 *o*-F of the R_F *trans* to I, $^3J_{F,Pt}$ = 505 Hz, $^3J_{F,F}$ = 30 Hz), −166.5 (t, 1 *p*-F of the R_F *trans* to P, $^3J_{F,F}$ = 19 Hz), −166.9 (m, 2 *m*-F of the R_F *trans* to P, $^3J_{F,F}$ = 20 Hz, $^5J_{F,P}$ = 10 Hz), −168.3 (pseudo t, 2 *m*-F of the R_F *trans* to I, $^4J_{F,Pt}$ = 138 Hz, mean $^3J_{F,F}$ = 24 Hz) −168.7 (t, 1 *p*-F of the R_F *trans* to I, $^3J_{F,F}$ = 19 Hz) ppm.

10-hydr. HRMS(−), exact mass for the anion $[C_{36}H_{21}F_{10}I_2OP_2Pt_2]^-$: 1364.8289; measured: *m/z*: 1364.8294 (M)$^-$. ^{1}H NMR (298 K, $(CD_3)_2CO$, 400 MHz): δ 7.96 (dd, 4H, *o*-Ph bonded to P^A, 10.4 Hz, 7.9 Hz), δ 7.81 (dd, 4H, *o*-Ph bonded to P^B, 12.4 Hz, 8.0 Hz), 7.54 (s, PO*H*, detected from ^{1}H EXSY spectrum, by its exchange with H_2O), 7.52 (t, 2H, *p*-Ph bonded to P^B, 7.4 Hz), 7.45 (pseudo t, 4H, *m*-Ph bonded to P^B, 7.4 Hz), 7.22 (t, 6H, *p*-Ph bonded to P^A, 7.2 Hz) 7.13 (pseudo t, 4H, *m*-Ph bonded to P^A, 7.2 Hz), 3.49 (m, 8H, NBu_4^+), 1.87 (m, 8H, NBu_4^+), 1.49 (pseudo sextet, 8H, 7.4

Hz, NBu_4^+), 1.03 (t, 12H, 7.4 Hz, NBu_4^+) ppm. ^{19}F NMR (298 K, $(CD_3)_2CO$, 376.5 MHz): δ −115.2 (pseudo t, 2 *o*-F of the R_F *trans* to P, $^3J_{F,Pt}$ = 345 Hz, $^3J_{F,F}$ = $^3J_{F,P}$ = 19 Hz), −116.7 (d, 2 *o*-F of the R_F *trans* to I, $^3J_{F,Pt}$ = 503 Hz, $^3J_{F,F}$ = 29 Hz), −166.7 (t, 1 *p*-F of the R_F *trans* to P, $^3J_{F,F}$ = 19 Hz), −167.0 (td, 2 *m*-F of the R_F *trans* to P, $^3J_{F,F}$ = 19 Hz, $^5J_{F,P}$ = 9 Hz), −168.2 (pseudo t, 2 *m*-F of the R_F *trans* to I, $^4J_{F,Pt}$ = 136 Hz, mean $^3J_{F,F}$ = 24 Hz) −169.0 (t, 1 *p*-F of the R_F *trans* to I, $^3J_{F,F}$ = 19 Hz) ppm.

Synthesis of [NBu4][(PPh2-pic)(RF)Pt(μ-I)(μ-PPh2)Pd(RF)I], 11. I_2 (0.037 g, 0.146 mmol) in CH_2Cl_2 (10 mL) was added dropwise to a yellow solution of **5** (0.200 g, 0.146 mmol) in CH_2Cl_2 (5 mL). The solution was stirred under nitrogen at room temperature for 20 h and then evaporated to dryness. The solid residue was recrystallized from acetone/*i*-PrOH (1 mL/5 mL). Complex **11** crystallized as a yellow solid which was filtered, washed with cold *i*-PrOH (2 × 0.5 mL), and dried. 0.125 g, 53% yield. Found: C, 42.29; H, 3.65; N, 1.88. $C_{58}H_{60}F_{10}I_2N_2O_2P_2PdPt$ requires C, 42.89; H, 3.72; N, 1.72. HRMS(−), exact mass for the anion $[C_{42}H_{24}F_{10}I_2NO_2P_2PdPt]^-$: 1381.7887 Da; measured: *m*/*z*: 1381.7895 (M)$^-$. ^{1}H NMR (298 K, $(CD_3)_2CO$, 400 MHz): δ 8.60 (broad d, 1H, H^2, 3.9 Hz), 7.89−7.79 (m, 6H, *o*-Ph bonded to P^B, H^4, H^5), 7.64−7.54 (m, 3H, *p*-Ph bonded to P^B, H^3), 7.51−7.38 (m, 8H, *o*-Ph bonded to P^A, *m*-Ph bonded to P^B), 7.06 (t, 2H, *p*-Ph bonded to P^A, 7.2 Hz), 6.88 (pseudo t, 4H, *m*-Ph bonded to P^A, 7.1 Hz), 3.49 (m, 8H, NBu_4^+), 1.87 (m, 8H, NBu_4^+), 1.49 (pseudo sextet, 8H, 7.4 Hz, NBu_4^+), 1.03 (t, 12H, 7.4 Hz, NBu_4^+) ppm. ^{19}F NMR (298 K, $(CD_3)_2CO$, 376.5 MHz): δ −112.2 (d, 2 *o*-F of the R_F *trans* to I, $^3J_{F,F}$ = 28 Hz), −115.5 (dd, 2 *o*-F of the R_F *trans* to P, $^3J_{F,Pt}$ = 256 Hz, $^3J_{F,F}$ = 24 Hz, $^4J_{F,P}$ = 17 Hz), −164.9 (t, 1 *p*-F of the R_F *trans* to P, $^3J_{F,F}$ = 19 Hz), −166.1 (m, 2 *m*-F of the R_F *trans* to P, $^3J_{F,F}$ = 24 Hz, $^3J_{F,F}$ = 19 Hz), −167.0 to −167.3 (m, 1 *p*-F of the R_F *trans* to I, 2 *m*-F of the R_F *trans* to I) ppm.

Synthesis of [NBu4][(RF)2Pt(μ-I)(μ-PPh2)PtI(Ph2P-acac)] (12). I_2 (0.035 g, 0.140 mmol) in CH_2Cl_2 (10 mL) was added dropwise to a colorless solution of $[NBu_4][(R_F)_2Pt(\mu\text{-}PPh_2)_2Pt(O,O'\text{-acac})]$ (**6**) (0.201 g, 0.140 mmol) in CH_2Cl_2 (20 mL), and the resulting mixture was stirred at room temperature for 20 h. The obtained yellow solution was evaporated to ca. 2 mL, $CHCl_3$ (8 mL) was added, and evaporated to ca. 6 mL. The mixture was stirred for 30 min, and **12** crystallized as a yellow solid which was filtered, washed with cold $CHCl_3$ (2× 1 mL), and dried. 0.168 g, 69% yield. Found: C, 40.26; H, 3.82; N, 1.18. $C_{57}H_{63}F_{10}I_2NO_2P_2Pt_2$ requires C, 40.51; H, 3.76; N, 0.83. HRMS(−), exact mass for the anion $[C_{41}H_{27}F_{10}I_2O_2P_2Pt_2]^-$: 1446.870 Da; measured: *m*/*z*: 1446.8720 (M)$^-$. ^{1}H NMR (298 K, $(CD_3)_2CO$, 400 MHz): δ 7.98 (dd, 4H, *o*-Ph bonded to P^A, 10.8 Hz, 8.5 Hz), 7.66 (dd, 4H, *o*-Ph bonded to P^B, 12.2 Hz, 7.3 Hz), 7.58 (t, 2H, *p*-Ph bonded to P^B, 6.9 Hz), 7.49 (pseudo t, 4H, *m*-Ph bonded to P^B, 7.3 Hz), 7.36−7.22 (m, 6H, *p*-Ph bonded to P^A, *m*-Ph bonded to P^A) 4.96 (d, 1H, C*H*, 2.0 Hz), 3.49 (m, 8H, NBu_4^+), 1.87 (m, 8H, NBu_4^+), 1.72 (s, 3H, (O═C)-CH_3)), 1.49 (pseudo sextet, 8H, 7.4 Hz, NBu_4^+), 1.40 (s, 3H, C═C−CH_3), 1.03 (t, 12H, 7.4 Hz, NBu_4^+) ppm. ^{19}F NMR (298 K, $(CD_3)_2CO$, 376.5 MHz): δ −115.3 (m, 2 *o*-F of the R_F *trans* to P, $^3J_{F,Pt}$ = 340 Hz, $^3J_{F,F}$ = $^3J_{F,P}$ = 18 Hz), −116.9 (d, 2 *o*-F of the R_F *trans* to I, $^3J_{F,Pt}$ = 497 Hz, $^3J_{F,F}$ = 29 Hz), −166.5 (t, 1 *p*-F of the R_F *trans* to P, $^3J_{F,F}$ = 19 Hz), −166.9 (td, 2 *m*-F of the R_F *trans* to P, $^3J_{F,F}$ = 19 Hz, $^5J_{F,P}$ = 9 Hz), −168.1 (pseudo t, 2 *m*-F of the R_F *trans* to I, $^4J_{F,Pt}$ = 137 Hz, mean $^3J_{F,F}$ = 24 Hz) −168.7 (t, 1 *p*-F of the R_F *trans* to I, $^3J_{F,F}$ = 19 Hz) ppm.

NMR Monitoring of the Reaction Solutions. An NMR tube kept at 268 K was charged with an acetone-d_6 solution of **1** (0.030 g, 0.024 mmol in 0.5 mL), solid NBu_4I (0.037 mg, 0.100 mmol), and solid I_2 (18 mg, 0.072 mmol) and vigorously shaken. The resulting red solution was put in the NMR probe precooled at 268 K, and multinuclear NMR spectra were recorded. The mixture revealed the immediate formation of **1-ox** that, under these conditions, was found stable at 268 K for at least one week. The same procedure was followed for (i) the monitoring of the reaction between **1** (0.030 g, 0.024 mmol in 0.5 mL), and solid I_2 (6.1 mg, 0.024 mmol) in acetone-d_6 at 298 K, which showed the transformation of **1-ox** into **7**; (ii) the monitoring of the reaction between **4** (0.030 g, 0.025 mmol in 0.5 mL), solid NBu_4I (0.037 mg, 0.100 mmol), and solid I_2 (18 mg, 0.072 mmol) in acetone-d_6 at 268 K, which showed the formation of **4-ox**; (iii) the monitoring of the reaction between **4** (0.030 g, 0.025 mmol in 0.5 mL), and solid I_2 (6.4 mg, 0.025 mmol) in anhydrous thf at 298 K, which showed the transformation of **4-ox** into **10**; (iv) the monitoring of the reaction between **6** (0.030 g, 0.025 mmol in 0.5 mL), solid NBu_4I (0.037 mg, 0.100 mmol), and solid I_2 (18 mg, 0.072 mmol) in acetone-d_6 at 268 K, which showed the formation of **6-ox**-*cis* and -*trans*; (v) the monitoring of the reaction between **6** (0.030 g, 0.025 mmol in 0.5 mL) and solid I_2 (6.4 mg, 0.025 mmol) in acetone-d_6 at 298 K, which showed the transformation of **6-ox** into **12**.

X-ray Structure Determinations. Crystal data and other details of the structure analyses are presented in Table S1. Suitable crystals for X-ray diffraction studies were obtained by slow diffusion of *n*-hexane into concentrated solutions of the complexes in 3 mL of Me_2CO or CH_2Cl_2. Crystals were mounted at the end of a quartz fiber. The radiation used in all cases was graphite monochromated $Mo_{K\alpha}$ (λ = 0.71073 Å). For **7**, **9**, and **11**, X-ray intensity data were collected on an Oxford Diffraction Xcalibur diffractometer. The diffraction frames were integrated and corrected from absorption by using the CrysAlis RED program.[74] For **12**, diffraction measurements were made on an Enraf-Nonius CAD-4 diffractometer. Diffracted intensities were measured in a hemisphere of reciprocal space. Three check reflections remeasured after every 300 ordinary reflections showed no decay of the diffracted intensities over the period of data collection. An absorption correction was applied based on 548 azimuthal scan data.

The structures were solved by Patterson and Fourier methods and refined by full-matrix least-squares on F^2 with SHELXL-97.[75] All non-hydrogen atoms were assigned anisotropic displacement parameters and refined without positional constraints, except as noted below. All hydrogen atoms were constrained to idealized geometries and assigned isotropic displacement parameters equal to 1.2 times the U_{iso} values of their attached parent atoms (1.5 times for the methyl hydrogen atoms). In the structures of **7**·2Me_2CO and **9**·Me_2CO·0.25*n*-C_6H_{14}, restraints were applied in the geometry of the acetone solvent and *n*-hexane molecules respectively. In the structure of **12**, the tetrabutylammonium cation was found to be very badly disordered, with two positions sharing some of the carbon atoms of the butyl "branches"; moreover, some of the nonshared carbon atoms are also disordered over two positions. Partial occupancy assignments and restraints in the geometry were used for this moiety. Full-matrix least-squares refinement of these models against F^2 converged to final residual indices given in Table S1.

■ ASSOCIATED CONTENT

Supporting Information

Crystallographic data of **7**·2Me_2CO, **9**·Me_2CO·0.25*n*-C_6H_{14}, **11**·CH_2Cl_2, and **12** (CIF format); NMR spectra of **1**−**5**, **7**, **10**−**12**, **1-ox**, **4-ox**, **6-ox**; HRMS spectrograms of **1**−**5**, **7**−**12**, **1-ox**, **4-ox**, **6-ox**. This material is available free of charge via Internet at http://pubs.acs.org

■ AUTHOR INFORMATION

Corresponding Author

*E-mail: cfortuno@unizar.es (C.F.); p.mastrorilli@poliba.it (P.M.).

Notes

The authors declare no competing financial interest.

■ ACKNOWLEDGMENTS

This work was supported by the Spanish MICINN (Project CTQ2008-06669-C02-01), the Ministerio de Economía y Competitividad (Project CTQ2012-35251), and the Cobierno de Aragón (Grupo de Consolidado: Química Inorgánica y de los Compuestos Organometálicos). A.A. gratefully acknowledges MICINN for a FPU grant. Italian MIUR (PRIN project n. 2009LR88XR) is also acknowledged for financial support.

REFERENCES

(1) Forniés, J.; Fortuño, C.; Ibáñez, S.; Martín, A.; Mastrorilli, P.; Gallo, V.; Tsipis, A. *Inorg. Chem.* **2013**, *52*, 1942−1953.
(2) Xu, L. M.; Li, B. J.; Yang, Z.; Shi, Z. J. *Chem. Soc. Rev.* **2010**, *39*, 712−733.
(3) Sehnal, P.; Taylor, R. J. K.; Fairlamb, I. J. S. *Chem. Rev.* **2010**, *110*, 824−889.
(4) Lyons, T. W.; Sanford, M. S. *Chem. Rev.* **2010**, *110*, 1147−1169.
(5) Canty, A. J. *Dalton Trans.* **2009**, 10409−10417.
(6) Khusnutdinova, J. R.; Rath, N. P.; Mirica, L. M. *J. Am. Chem. Soc.* **2010**, *132*, 7303−7305.
(7) Crespo, M.; Anderson, C. M.; Kfoury, N.; Font-Bardia, M.; Calvet, T. *Organometallics* **2012**, *31*, 4401−4404.
(8) Tang, F.; Zhang, Y.; Rath, N. P.; Mirica, L. M. *Organometallics* **2012**, *31*, 6690−6696.
(9) Julia-Hernández, F.; Arcas, A.; Vicente, J. *Chem.—Eur. J.* **2012**, *18*, 7780−7786.
(10) Zhang, H.; Lei, A. *Dalton Trans* **2011**, *40*, 8745−8754.
(11) Ball, N. D.; Gary, J. B.; Ye, Y.; Sanford, M. S. *J. Am. Chem. Soc.* **2011**, *133*, 7577−7584.
(12) Sierra, D.; Cao, P.; Cabrera, J.; Padilla, R.; Rominger, F.; Limbach, M. *Organometallics* **2011**, *30*, 1885−1895.
(13) Vicente, J.; Arcas, A.; Juliá-Hernández, F.; Bautista, D. *Inorg. Chem.* **2011**, *50*, 5339−5341.
(14) Lanci, M. P.; Remy, M. S.; Lao, D. B.; Sanford, M. S.; Mayer, J. M. *Organometallics* **2011**, *30*, 3704−3707.
(15) Yahav-Levi, A.; Goldberg, I.; Vigalok, A.; Vedernikov, A. N. *Chem. Commun.* **2010**, *46*, 3324−3326.
(16) Vicente, J.; Arcas, A.; Juliá-Hernández, F.; Bautista, D. *Angew. Chem., Int. Ed.* **2011**, *50*, 6896−6899.
(17) Zhao, X.; Dong, V. M. *Angew. Chem., Int. Ed.* **2011**, *50*, 932−934.
(18) Racowski, J. M.; Gary, J. B.; Sanford, M. S. *Angew. Chem., Int. Ed.* **2012**, *51*, 3414−3417.
(19) Ariafard, A.; Hyland, C. J. T.; Canty, A. J.; Sharma, M.; Brookes, N. J. *Inorg. Chem.* **2010**, *49*, 11249−11253.
(20) Ariafard, A.; Hyland, C. J. T.; Canty, A. J.; Sharma, M.; Yates, B. F. *Inorg. Chem.* **2011**, *50*, 6449−6457.
(21) Deprez, N. R.; Sanford, M. S. *J. Am. Chem. Soc.* **2009**, *131*, 11234−11241.
(22) Penno, D.; Estevan, F.; Fernández, E.; Hirva, P.; Lahuerta, P.; Sanaú, M.; Ubeda, M. A. *Organometallics* **2011**, *30*, 2083−2094.
(23) Powers, D. C.; Ritter, T. *Nat. Chem.* **2009**, *1*, 302−309.
(24) Matsumoto, K.; Ochiai, M. *Coord. Chem. Rev.* **2002**, *231*, 229−238.
(25) Canty, A. J.; Gardiner, M. G.; Jones, R. C.; Rodemannn, T.; Sharma, M. *J. Am. Chem. Soc.* **2009**, *131*, 7236−7237.
(26) Whitfield, S. R.; Sanford, M. S. *Organometallics* **2008**, *27*, 1683−1689.
(27) Powers, D. C.; Lee, E.; Ariafard, A.; Sanford, M. S.; Yates, B. F.; Canty, A. J.; Ritter, T. *J. Am. Chem. Soc.* **2012**, *134*, 12002−12009.
(28) Powers, D. C.; Ritter, T. *Acc. Chem. Res.* **2012**, *45*, 840−850.
(29) Hickman, A. J.; Sanford, M. S. *Nature* **2012**, *484*, 177−185.
(30) Wilson, J. J.; Lippard, S. J. *Inorg. Chem.* **2012**, *51*, 9852−9864.
(31) Sicilia, V.; Forniés, J.; Casas, J. M.; Martín, A.; López, J. A.; Larraz, C.; Borja, P.; Ovejero, C.; Tordera, D.; Bolink, H. *Inorg. Chem.* **2012**, *51*, 3427−3435.
(32) Ibáñez, S.; Estevan, F.; Hirva, P.; Sanaú, M.; Ubeda, M. A. *Organometallics* **2012**, *31*, 8098−8108.
(33) Chaouche, N.; Forniés, J.; Fortuño, C.; Kribii, A.; Martín, A.; Karipidis, P.; Tsipis, A. C.; Tsipis, C. A. *Organometallics* **2004**, *23*, 1797−1810.
(34) Arias, A.; Forniés, J.; Fortuño, C.; Martín, A.; Latronico, M.; Mastrorilli, P.; Todisco, S.; Gallo, V. *Inorg. Chem.* **2012**, *51*, 12682−12696.
(35) Ara, I.; Chaouche, N.; Forniés, J.; Fortuño, C.; Kribii, A.; Tsipis, A. C. *Organometallics* **2006**, *25*, 1084−1091.
(36) Alonso, E.; Casas, J. M.; Cotton, F. A.; Feng, X. J.; Forniés, J.; Fortuño, C.; Tomás, M. *Inorg. Chem.* **1999**, *38*, 5034−5040.
(37) Forniés, J.; Fortuño, C.; Navarro, R.; Martínez, F.; Welch, A. J. *J. Organomet. Chem.* **1990**, *394*, 643−658.
(38) Alonso, E.; Forniés, J.; Fortuño, C.; Tomás, M. *J. Chem. Soc., Dalton Trans.* **1995**, 3777−3784.
(39) Alonso, E.; Forniés, J.; Fortuño, C.; Martín, A.; Orpen, A. G. *Organometallics* **2003**, *22*, 5011−5019.
(40) Ara, I.; Chaouche, N.; Forniés, J.; Fortuño, C.; Kribii, A.; Martín, A. *Eur. J. Inorg. Chem.* **2005**, 3894−3901.
(41) Berenguer, J. R.; Chaouche, N.; Forniés, J.; Fortuño, C.; Martín, A. *New J. Chem.* **2006**, *30*, 473−478.
(42) Ara, I.; Forniés, J.; Fortuño, C.; Ibáñez, S.; Martín, A.; Mastrorilli, P.; Gallo, V. *Inorg. Chem.* **2008**, *47*, 9069−9080.
(43) Forniés, J.; Fortuño, C.; Ibáñez, S.; Martín, A.; Mastrorilli, P.; Gallo, V. *Inorg. Chem.* **2011**, *50*, 10798−10809.
(44) Alonso, E.; Casas, J. M.; Forniés, J.; Fortuño, C.; Martín, A.; Orpen, A. G.; Tsipis, C. A.; Tsipis, A. C. *Organometallics* **2001**, *20*, 5571−5582.
(45) Falvello, L. R.; Forniés, J.; Fortuño, C.; Durán, F.; Martín, A. *Organometallics* **2002**, *21*, 2226−2234.
(46) Mastrorilli, P. *Eur. J. Inorg. Chem.* **2008**, 4835−4850.
(47) Carty, A. J.; MacLaughlin, S. A.; Nucciarone, D. *Phosphorus-31 NMR Spectroscopy in Stereochemical Analysis*; VCH: New York, 1987.
(48) de la Mora, J. F.; Van Berkel, G. J.; Enke, C. G.; Cole, R. B.; Martinez-Sanchez, M.; Fenn, J. B. *J. Mass Spectrom.* **2000**, *35*, 939−952.
(49) Kebarle, P. *J. Mass Spectrom.* **2000**, *35*, 804−817.
(50) The HRMS(+) peak is compatible also with a Pt(II))Pt(IV) formulation of the oxidised cations, but this would be in contrast with the tendency of Pt(IV) to give almost invariably octahedral six-coordinated species. On the other hand, phosphanido bridged Pt(III) Pt(III) systems endowed with a metal bond have long been known: refs 35, 36, 42−44.
(51) The HRMS(+) analyses of **1**−**5** were all carried out using acetonitrile solutions of the complexes having approximately the same molar concentration.
(52) Bender, R.; Okio, C.; Welter, R.; Braunstein, P. *Dalton Trans.* **2009**, 4901−4907.
(53) Ara, I.; Chaouche, N.; Forniés, J.; Fortuño, C.; Kribii, A.; Tsipis, A. C.; Tsipis, C. A. *Inorg. Chim. Acta* **2005**, *358*, 1377−1385.
(54) Forniés, J.; Fortuño, C.; Ibáñez, S.; Martín, A. *Inorg. Chem.* **2006**, *45*, 4850−4858.
(55) De Pascali, S. A.; Papadia, P.; Capoccia, S.; Marchiò, L.; Lanfranchi, M.; Ciccarese, A.; Fanizzi, F. P. *Dalton Trans.* **2009**, 7786−7795.
(56) Alonso, E.; Forniés, J.; Fortuño, C.; Martín, A.; Rosair, G. M.; Welch, A. J. *Inorg. Chem.* **1997**, *36*, 4426−4431.
(57) Forniés, J.; Fortuño, C.; Gil, R.; Martín, A. *Inorg. Chem.* **2005**, *44*, 9534−9541.
(58) Forniés, J.; Fortuño, C.; Ibáñez, S.; Martín, A. *Inorg. Chem.* **2008**, *47*, 5978−5987.
(59) Throughout the paper, the calculated (exact mass) and the experimental (accurate) m/z values have been compared considering the principal ion (which gives the most intense peak) of the isotope pattern.
(60) A different behaviour between the benzoquinolinate and the 8-hydroxyquinolinate systems was found comparing the dynamics in solution of **B-ox** with that of **1-ox**: while in the case of **B-ox** the exchange between two phenyl rings bonded to different P atoms was observed at 298 K in acetone-d_6,[34] in the case of **1-ox** no exchanges were observed by ^{1}H NOESY experiments carried out in the same conditions. A rationale for this different behaviour may be the different strength of the P-O vs P-C bond, the former being more stable, which manifests itself in an irreversible P-O bond formation (8-hydroxyquinolinate system) in contrast to the reversible P-C bond formation (benzoquinolinate system).
(61) An example of coordinated PPh_2I arising from reaction of a phosphanido bridged dirhenium complex with I_2 is reported in: Flörke, U.; Haupt, H.-J. *Acta Crystallogr.* **1991**, *C47*, 1535−1537. while a PPh_2I Nb complex is described in: Antiñolo, A.; García-Yuste, S.;

Otero, A.; Pérez-Flores, J. C.; Reguillo-Carmona, R.; Rodríguez, A. M.; Villaseñor, E. *Organometallics* **2006**, *25*, 1310−1316.
(62) The iododiphenylphosphane complex $NBu_4[(R_F)_2Pt(\mu\text{-}PPh_2)(\mu\text{-}I)Pt(PPh_2I)I]$ accounted for the remaining 15%.
(63) A related irreversible trans to cis isomerization of a diiodoPt(IV) complex has been described in Yahav, A.; Goldberg, I.; Vigalok, A. *Organometallics* **2005**, *24*, 5654−5659.
(64) Yahav-Levi, A.; Goldberg, I.; Vigalok, A.; Vedemikov, A. N. *J. Am. Chem. Soc.* **2008**, *130*, 724−731.
(65) Yahav, A.; Goldberg, I.; Vigalok, A. *Organometallics* **2005**, *24*, 5654−5659.
(66) Yagyu, T.; Ohashi, J.; Maeda, M. *Organometallics* **2007**, *26*, 2383−2391.
(67) Macgregor, S. A. *Chem. Soc. Rev.* **2007**, *36*, 67−76.
(68) Archambault, C.; Bender, R.; Braunstein, P.; Decian, A.; Fischer, J. *Chem. Commun.* **1996**, 2729−2730.
(69) Cabeza, J. A.; del Río, I.; Riera, V.; García-Granda, S.; Sanni, S. B. *Organometallics* **1997**, *16*, 1743−1748.
(70) Albinati, A.; Filippi, V.; Leoni, P.; Marchetti, L.; Pasquali, M.; Passarelli, V. *Chem. Commun.* **2005**, 2155−2157.
(71) Chaouche, N.; Forniés, J.; Fortuño, C.; Kribii, A.; Martín, A. *J. Organomet. Chem.* **2007**, *692*, 1168−1172.
(72) Forniés, J.; Fortuño, C.; Ibáñez, S.; Martín, A.; Tsipis, A. C.; Tsipis, C. A. *Angew. Chem., Int. Ed.* **2005**, *44*, 2407−2410.
(73) Hartwell, G. E.; Lawrence, R. V.; Smas, M. J. *J. Chem. Soc., Chem. Commun.* **1970**, 912.
(74) *CrysAlisRED, Program for X-ray CCD Camera Data Reduction*, Version 1.171.32.19; Oxford Diffraction Ltd.: Oxford, UK, 2008.
(75) Sheldrick, G. M. *SHELXL-97 A Program for Crystal Structure Determination*; University of Gottingen: Germany, 1997.